

Theoretical Studies on the Addition of Polymetallic Lithium Organocuprate Clusters to Acetylene. Cooperative Effects of Metals in a Trap-and-Bite Reaction Pathway

Eiichi Nakamura,^{*,†} Seiji Mori,[†] Masaharu Nakamura,[†] and Keiji Morokuma^{*,‡}

Contribution from the Department of Chemistry, The University of Tokyo, Bunkyo-ku, Tokyo 152, Japan, and Cherry L. Emerson Center for Scientific Computation and Department of Chemistry, Emory University, Atlanta, Georgia 30322

Received December 6, 1996[⊗]

Abstract: *Ab initio* and density functional theoretical investigations into the nature of the reaction of acetylene with noncluster organocuprate reagents, MeCu, Me₂Cu⁻, and lithium organocuprate cluster reagents, Me₂CuLi, Me₂CuLi·LiCl, and (Me₂CuLi)₂ were carried out, and the function of the mixed metal cluster was probed. Intermediates transition structures (TSs) as well as the structures on the intrinsic reaction coordinate in the C–C bond forming stage of the reaction of lithium cuprate clusters have been calculated with the *ab initio* method (MP2) and density functional method (B3LYP) using all-electron basis sets for copper. The addition reaction of the simple organocuprate reagent, MeCu, can be viewed as a simple four-centered addition reaction consisting of nucleophilic addition of an anionic methyl group, while the addition of the cuprate reagent, Me₂Cu⁻, involves transfer of negative charge to the acetylene via the copper atom. In the cluster reaction of Me₂CuLi·LiCl, the lithium atom in the cluster stabilizes the developing negative charge on the acetylene moiety and assists the electron flow from the copper atom. Reductive elimination of the transient Cu(III) species initially gives a 1-propenyllithium-like structure intermediate (nonstationary point), which then undergoes intramolecular transmetalation to give the final product, 1-propenylcopper. Essentially the same mechanism operates also with Me₂CuLi and (Me₂CuLi)₂, indicating that the Li–Me–Cu–Me moiety incorporated in the mixed organocuprate cluster is essential for the reaction. Experiments showed that the strong solvation of the lithium atom with a crown ether, which sequesters the lithium cation from the cluster, strongly decelerates the carbocupration reaction. Thus, theory and experiments revealed the cooperative function of lithium and copper atoms in the cuprate reactions.

Introduction

“Of all the transition-metal organometallic reagents developed for application to organic synthesis, organocuprate complexes are by far the most heavily used and enthusiastically accepted by the synthetic organic chemist”.^{1,2} However, the nature of the reactive species and their reaction pathway are not yet fully understood. In the 1960s, House demonstrated that the reactive species in the organocuprate reactions are a species having the “R₂CuLi” stoichiometry.³ The simplest organocuprate species, RCu, is not reactive enough to be synthetically useful. After many years of synthetic exploration, there exists now a variety of cuprate reagents of the general formula [R₁R₂Cu]⁻M⁺, and the reactivity of the cuprate reagents have been tuned by

judicious selection of the “countercation” M⁺. For instance, upon complexation with crown ether, the R₂CuLi reagent loses its ability to undergo conjugate addition to enones⁴ and to add to acetylenes (vide infra), while cuprates having a Lewis acidic metal as M⁺ (M⁺ = Zn(II),⁵ Ti(IV),⁶ Zr(IV),⁶ etc. as well as neutral additives as such as BF₃,⁷ Me₃SiCl,⁸ etc.) often exhibit better selectivities than the lithium cuprates. The exact role of M⁺, however, remains to be understood.

The prototypical reagent R₂CuLi exists predominantly as a dimer in solution, as revealed by various physical measurements.⁹ The dimer has been suggested to have a cyclic structure **A** consisting of alternating Li and Cu bridged by pentacoordi-

[†] The University of Tokyo.

[‡] Emory University.

[⊗] Abstract published in *Advance ACS Abstracts*, May 1, 1997.

(1) Collman, J. P.; Hegedus, L. S.; Norton, J. R.; Finke, R. G. *Principles and Applications of Organotransition Metal Chemistry*, 2nd ed.; University Sciencebooks: Mill Valley, CA, 1987; Chapter 14.

(2) (a) Reviews: Posner, G. H. *Organic Reactions* **1972**, *19*, 1–113. Normant, J. F. *Synthesis* **1972**, 63–80. Lipshutz, B. H. Sengupta, S. R. *Organic Reactions* **1992**, *41*, 135–631. *Organocuprate Reagents*; Taylor, R. J. K., Ed.; Oxford University Press: UK, 1994. van Koten, G.; Noltes, J. G. *Comprehensive Organometallic Chemistry*; Wilkinson, G., Stone, F. G. A., Eds.; Pergamon: Oxford, 1982; Vol. 2, pp 709–763. van Koten, G.; James, S. L.; Jastrzebski, J. T. B. H. *Comprehensive Organometallic Chemistry II*; Abel, E. W., Stone, F. G. A., Wilkinson, G., Eds.; Pergamon: Oxford, 1995; Vol. 3, pp 57–133. Lipshutz, B. H. *Comprehensive Organometallic Chemistry II*; Abel, E. W., Stone, F. G. A., Wilkinson, G., Eds.; Pergamon: Oxford, 1995; Vol. 12, pp 59–130. (b) For a unique chemistry of organocuprates in fullerene chemistry, see: Sawamura, M.; Iikura, H.; Nakamura, E. *J. Am. Chem. Soc.* **1996**, *118*, 12850–12851.

(3) House, H. O.; Respass, W. L.; Whitesides, G. M. *J. Org. Chem.* **1966**, *31*, 3128–3141. Cf.: Gilman, H.; Jones, R. G.; Woods, L. A. *J. Org. Chem.* **1952**, *17*, 1630–1634.

(4) Ouannes, C.; Dressaire, G.; Langlois, Y. *Tetrahedron Lett.* **1977**, *10*, 815–818.

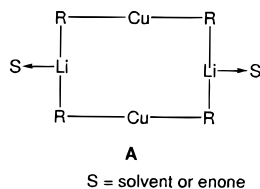
(5) Nakamura, E.; Sekiya, K.; Arai, M.; Aoki, S. *J. Am. Chem. Soc.* **1989**, *111*, 3091–3093. Arai, M.; Kawasuji, T.; Nakamura, E. *J. Org. Chem.* **1993**, *58*, 5121–5129.

(6) (a) Arai, M.; Nakamura, E.; Lipshutz, B. H. *J. Org. Chem.* **1991**, *56*, 5489–5491. (b) Zr(IV): Lipshutz, B. H.; Ellsworth, E. L. *J. Am. Chem. Soc.* **1990**, *112*, 7440–7441.

(7) Yamamoto, Y. *Angew. Chem., Int. Ed. Engl.* **1986**, *25*, 947–959. Lipshutz, B. H.; Ellsworth, E. L.; Siahaan, T. J. *J. Am. Chem. Soc.* **1989**, *111*, 1351–1358.

(8) (a) Chuit, C.; Foulon, J. P.; Normant, J. F. *Tetrahedron* **1980**, *36*, 2305–2310. (b) Nakamura, E.; Kuwajima, I. *J. Am. Chem. Soc.* **1984**, *106*, 3368–3370. Horiguchi, Y.; Matsuzawa, S.; Nakamura, E.; Kuwajima, I. *Tetrahedron Lett.* **1986**, *27*, 4025–4028. Nakamura, E.; Matsuzawa, S.; Horiguchi, Y.; Kuwajima, I. *Tetrahedron Lett.* **1986**, *27*, 4029–4032. (c) Corey, E. J.; Boaz, N. W. *Tetrahedron Lett.* **1985**, *26*, 6015–6018 and 6019–6022. (d) Alexakis, A.; Berlan, J.; Besace, Y. *Tetrahedron Lett.* **1986**, *27*, 1047–1050. (e) Johnson, C. R.; Marren, T. J. *Tetrahedron Lett.* **1987**, *28*, 27–30. (f) Nakamura, E. In *Organocuprate Reagents*; Taylor, R. J. K., Ed.; Oxford University Press: UK, 1994; Chapter 6, pp 129–142. (g) Rate acceleration of Me₃SiI, see: Eriksson, M.; Johansson, A.; Nilsson, M.; Olsson, T. *J. Am. Chem. Soc.* **1996**, *118*, 10904–10905.

nated alkyl or aryl groups, which was identified in the crystals of several cuprates (e.g., R = Ph, Me₃SiCH₂).¹⁰ NMR studies on ¹H, ¹³C, and ⁷Li nuclei carried out for reagents of the R₂-CuLi stoichiometry also supported the presence of the dimeric aggregate in an ethereal solution.^{11,12}



In the kinetic studies of the conjugate addition and S_N2 alkylation of alkyl and aryl halides,^{9b,13,14} the reaction rates were found to be first order to both the substrate and the dimer (R₂-CuLi)₂. Thus, the dimer R₂CuLi has been suggested to be a kinetically reactive species. In the conjugate addition reaction, a kinetically observable cuprate/enone complex forms first, exists in equilibrium with the dimer and the substrate, and then affords the final product.¹⁵ Recent NMR studies successfully detected what are likely to be this kinetically observable complexes^{16,17} and revealed that they are π-complexes between a cuprate and an enone substrate bound together by donation/backdonation interaction. The NMR spin coupling studies showed that this π-complex assumes characters which are consistent with the long discussed Cu(III) intermediate.¹⁸ The recent isolation and elucidation of the crystal structures of stable Cu(III) organometallics^{19,20} (e.g., [(CF₃)₄Cu]⁻) gave a strong support to the possible intervention of a Cu(III) intermediates in cuprate addition.²¹

(9) (a) van Koten, G.; Noltes, J. G. *J. Chem. Soc., Chem. Commun.* **1972**, 940–941. (b) Pearson, R. G.; Gregory, C. D. *J. Am. Chem. Soc.* **1976**, *98*, 4098–4104.

(10) (a) van Koten, G.; Jastrzebski, J. T. B. H.; Muller, F.; Stam, C. H. *J. Am. Chem. Soc.* **1985**, *107*, 697–698. (b) Lorenzen, N. P.; Weiss, E. *Angew. Chem., Int. Ed. Engl.* **1990**, *29*, 300–302. (c) Olmstead, M. M.; Power, P. P. *Organometallics* **1990**, *9*, 1720–1722. (d) Olmstead, M. M.; Power, P. P. *J. Am. Chem. Soc.* **1990**, *112*, 8008–8014.

(11) Bertz, S. H.; Vellekoop, A. S.; Smith, R. A. J.; Snyder, J. P. *Organometallics* **1995**, *14*, 1213–1220.

(12) (a) Ashby, E. C.; Watkins, J. J. *J. Am. Chem. Soc.* **1977**, *99*, 5312–5317. (b) van Koten, G.; Noltes, J. G. *J. Organomet. Chem.* **1979**, *174*, 367–387. (c) Lipshutz, B. H.; Kozlowski, J. A.; Breneman, C. M. *J. Am. Chem. Soc.* **1985**, *107*, 3197–3204.

(13) Johnson, C. R.; Dutra, G. A. *J. Am. Chem. Soc.* **1973**, *95*, 7783–7787.

(14) Spanenberg, W. J.; Snell, B. E.; Su, M.-C. *Microchem. J.* **1993**, *47*, 79–89.

(15) Krauss, S. R.; Smith, S. G. *J. Am. Chem. Soc.* **1981**, *103*, 141–148.

(16) (a) Hallnemo, G.; Olsson, T.; Ullenius, C. *J. Organomet. Chem.* **1984**, *265*, C22–24. (b) Ullenius, C.; Christenson, B. *Pure Appl. Chem.* **1988**, 57–64.

(17) (a) Bertz, S. H.; Smith, R. A. J. *J. Am. Chem. Soc.* **1989**, *111*, 8276–8277. (b) Vellekoop, A. S.; Smith, R. A. J. *J. Am. Chem. Soc.* **1994**, *116*, 2902–2913.

(18) (a) Krause, N.; Wagner, R.; Gerold, A. *J. Am. Chem. Soc.* **1994**, *116*, 381–382. (b) Nilsson, K.; Ullenius, C.; Krause, N. *J. Am. Chem. Soc.* **1996**, *118*, 4194–4195.

(19) Willert-Porada, M. A.; Burton, D. J.; Baenziger, N. C. *J. Chem. Soc., Chem. Commun.* **1989**, 1633–1634. Neumann, D.; Roy, T.; Tebbe, K.-F.; Crump, W. *Angew. Chem., Int. Ed. Engl.* **1993**, *32*, 1482–1483. Eujen, R.; Hoge, B.; Brauer, D. J. *J. Organomet. Chem.* **1996**, *519*, 7–20.

(20) Kaupp, M.; von Schnering, H. G. *Angew. Chem., Int. Ed. Engl.* **1995**, *34*, 986.

(21) Appropriateness of the use of Cu(III) formality has been questioned (Snyder, J. P. *Angew. Chem., Int. Ed. Engl.* **1995**, *34*, 80–81) on the basis of the calculated electron density, which is far less positive (~+1) than the formal charge of +3, and this challenge has been discussed from the more standard inorganic viewpoint (cf. ref 20 and Snyder, J. P. *Angew. Chem., Int. Ed. Engl.* **1995**, *34*, 986–987). As the Snyder proposal would also pose problems in the use of the fundamental terminology such as “reductive elimination”, we use here the conventional formal oxidation nomenclature.

A number of cuprate reagents of monomeric stoichiometry, R₂CuLi·LiX (or R₂Cu(X)Li₂), are currently used in organic synthesis. It is important to note that, the synthetic copper reagents being prepared by the reaction of RLi with Cu(I) halides, they are almost always the reagents of R₂CuLi·LiX stoichiometry (X = I,^{11,22} Br,^{23,24} and Cl²⁵). The kinetic studies on conjugate addition¹⁵ and the alkylation reactions^{9b,13,14} indicated that the dimeric R₂CuLi remains to be a kinetically active species even in the presence of LiI, though the reaction rates were slightly affected by LiI.^{17a} The small LiI effects have been attributed to the high equilibrium concentration of a pair of cyclic dimers, (Me₂CuLi)₂ + (LiI)₂ in an ether solution of the “Me₂CuLi·LiI” reagent.¹¹ Very recent molecular weight determination indicated that Me₂CuLi·LiI in THF exists in the monomeric form.²²

As summarized above, a dimeric cluster exists in solution and takes part in the C–C bond forming reaction (e.g., conjugate addition and alkylation reaction). However, there is little understanding of the function of the cluster structure in cuprate chemistry. In light of the importance of cuprate chemistry and the paucity of information at the molecular level of understanding of clusters, we have carried out quantum mechanical studies on the dynamic behavior of cluster and noncluster organocuprates by *ab initio* molecular orbital and density functional (DF) methods. We have studied the reactions of three prototypical clusters, Me₂CuLi, Me₂CuLi·LiCl, and (Me₂CuLi)₂ as well as the simplest noncluster compounds, MeCu and Me₂Cu⁻, in order to address to the fundamental question: what is the role of clusters in organocuprate chemistry.

In this and the accompanying articles,²⁶ we will describe the first systematic theoretical studies on the reaction pathways of the polymetallic lithium organocuprate clusters reacting with C–C multiple bonds. This article describes (1) 1,2-addition of cuprates to acetylene along with a discussion on cuprate models and computational methods and (2) the conjugate addition of bis-, tri-, and tetrametallic cuprate clusters to acrolein. While different in the details of the reaction course, the two reactions were found to share in common important mechanistic features, a “trap-and-bite” reaction pathway realized by cooperation of the lithium and copper atoms. Though our studies were mainly focused on the process involving the crucial C–C bond forming process, and the reaction pathway prior to the C–C bond formation was also made.

The description of the theoretical work will be preceded by two sections dealing with the experimental background as well as some new experimental results as to the role of the lithium atom in the cuprate cluster. Comparison of theoretical methods as applied to dynamic behavior of organocopper reagents is

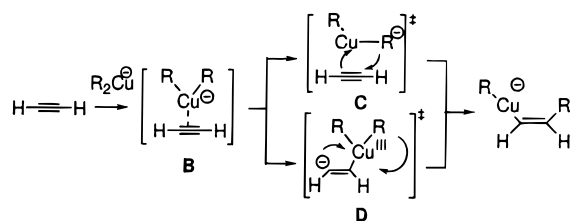
(22) Gerold, A.; Jastrzebski, J. T. B. H.; Kronenburg, C. M. P.; Krause, N.; van Koten, G. *Angew. Chem., Int. Ed. Engl.* **1997**, *36*, 755–757.

(23) (a) House, H. O.; Chu, C.-Y.; Wilkins, J. M.; Umen, M. J. *J. Org. Chem.* **1975**, *10*, 1460–1469. (b) Westmijze, H.; Kleijn, H.; Vermeer, P. *Tetrahedron Lett.* **1977**, *23*, 2023–2026. (c) Bertz, S. H.; Fairchild, E. H. *Encyclopedia of Reagents for Organic Synthesis*; Paquette, L. A., Ed.; John & Wiley: Chichester, 1995; Vol. 2, pp 1312–1315.

(24) Bertz, S. H.; Dabbagh, G. *J. Org. Chem.* **1984**, *49*, 1119–1122. Bertz, S. H.; *J. Am. Chem. Soc.* **1990**, *112*, 4031–4032. Bertz, S. H.; Fairchild, E. H. *Encyclopedia of Reagents for Organic Synthesis*; Paquette, L. A., Ed.; John & Wiley: Chichester, 1995; Vol. 2, pp 1346–1349.

(25) Bertz, S. H.; Fairchild, E. H. *Encyclopedia of Reagents for Organic Synthesis*; Paquette, L. A. Ed.; John & Wiley: Chichester, 1995; Vol. 2, pp 1324–1326. See, also: (a) stoichiometric reagents: Bertz, S. H.; Gibson, C. P.; Dabbagh, G. *Tetrahedron Lett.* **1987**, *28*, 4251–4254. Lipshutz, B. H.; Stevens, K. L.; James, B.; Pavlovich, J. G.; Snyder, J. P. *J. Am. Chem. Soc.* **1996**, *118*, 6796–6797. (b) Catalytic reagents: Tamura, M.; Kochi, J. *Synthesis* **1971**, 303–305. Giner, J.-L.; Margot, C.; Djerassi, C. *J. Org. Chem.* **1989**, *54*, 2117–2125. Schlosser, M.; Bossert, H. *Tetrahedron* **1991**, *47*, 6287–6292.

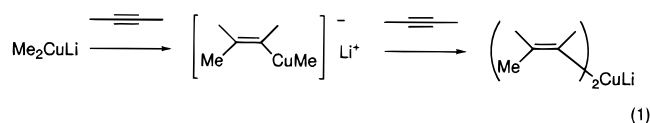
(26) Nakamura, E.; Mori, S.; Morokuma, K. *J. Am. Chem. Soc.* **1997**, *119*, 4900–4910.

Scheme 1. Schematic Representation of Two Conventional Mechanisms of Addition of R_2Cu^- to Acetylene

summarized in Appendix. This crucial information has been lacking in the literature.

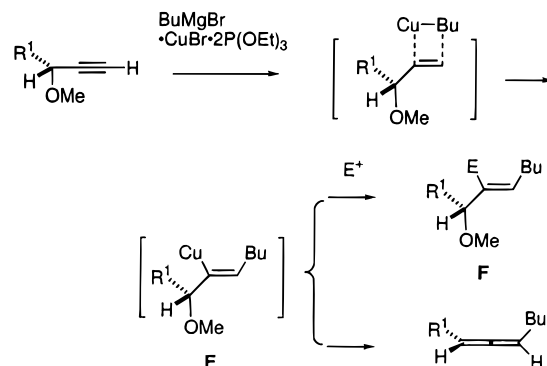
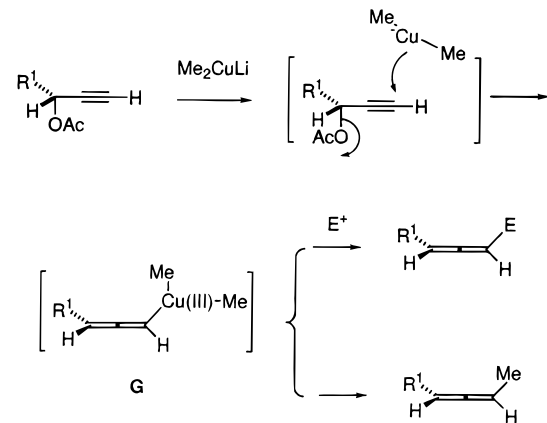
Acetylene Carbocupration. Background

Among various reactions of cuprates, we have selected the 1,2-addition of a methyl cuprate reagent to acetylene as the initial target of our studies (eq 1).^{27–29} The reaction is highly characteristic of organocopper chemistry and has provided uniquely effective entries to stereodefined vinyl metallic reagents starting from readily available acetylenic substrates. A related reaction of carbocupration of cyclopropenes provided a useful asymmetric transformation.³⁰ The simplicity of the reaction was also attractive: acetylene is the simplest among various electrophilic substrates in cuprate reactions, and the reaction mode is well defined (*cis* addition).²⁷ In order to clarify the role of each component of lithium organocuprate clusters, we studied the reactions of cluster and noncluster cuprates.



There have been two simplified mechanistic schemes proposed for the reaction of a cuprate with acetylene (Scheme 1).³¹ Regardless of the mechanism, a π -complex **B** is considered to form initially. In the first mechanism, the methyl group donates electrons to the acetylene leading to the straightforward four-centered addition reaction (**C**),³² and the Cu(I) oxidation state is maintained during the reaction. In the second one, the copper atom donates electrons to the acetylene by $d-\pi^*$ electron donation.³³ This would lead to a transition state such as **D**, from which the product forms with migration of the copper atom.

The two lines of contrasting experimental results on propargyl methyl ether (Scheme 2)³² and propargylic acetate³⁴ (Scheme 3) have been taken as support of each mechanism. In the methyl ether case, the vinyl copper product **E** has been identified chemically by electrophilic trapping. The reaction is therefore considered to have proceeded via the first mechanism. In the acetate reaction,^{34a} an allenyl Cu(III) intermediate **G** was

Scheme 2**Scheme 3**

chemically identified also by electrophilic trapping, which was taken to suggest a nucleophilic attack of Me_2Cu^- to the terminal carbon. In the absence of an external electrophile, the intermediate in each case decomposed to give an allenyl product by either 1,2-elimination or reductive elimination. Though these schemes are rational by themselves, it is puzzling why the initial attack point of the copper changes so dramatically by a mere change of the leaving group.

Computational Methods

General Methods. We used Gaussian 94 programs for all *ab initio* and DF calculations.³⁵ The *ab initio* Hartree–Fock (RHF) and RMP2-(FC) methods³⁶ were employed first for the studies on the reaction pathway of the $Me_2CuLi \cdot LiCl$ complex. The basis set used for the *ab initio* calculations (denoted as 631WH) consists of the Wachters (62111111/411111/311) contracted all-electron basis set³⁷ with one diffuse *d* function of Hay³⁸ for copper and 6-31G(d)³⁹ for the rest. For the $Me_2CuLi \cdot LiCl$ reaction, which was studied most extensively, intrinsic reaction coordinate (IRC) analysis⁴⁰ was performed near the

(27) Review: Normant, J. F. Alexakis, A. *Synthesis* **1981**, 841–870.

(28) Although the reaction takes place in two stages to incorporate two acetylene molecules into a cuprate species to give dipropenylcuprate (eq 1), we modeled only the first stage. In light of the results described later, the second stage will proceed in a similar manner.

(29) Alexakis, A.; Normant, J.; Villieras, J. *Tetrahedron Lett.* **1976**, 38, 3461–3462.

(30) Nakamura, E.; Isaka, M.; Matsuzawa, S. *J. Am. Chem. Soc.* **1988**, *110*, 1297–1298.

(31) Cf. Negishi, E.; Takahashi, T. *Synthesis* **1988**, 1–19.

(32) Alexakis, A.; Marek, I.; Mangeney, P.; Normant, J. F. *J. Am. Chem. Soc.* **1990**, *112*, 8042–8047.

(33) Corey, E. J.; Boaz, N. W. *Tetrahedron Lett.* **1984**, 25, 3063–3066.

(34) (a) Luche, J. L.; Barreiro, E.; Dollat, J. M.; Crabbé, P. *Tetrahedron Lett.* **1975**, 4615–4618. Dollat, J.-M.; Luche, J.-L.; Crabbé, P. *J. Chem. Soc. Chem. Commun.* **1977**, 761–762. (b) Vermeer, P.; Meijer, J.; Brandsma, L. *Rec. Trav. Chim. Pays-Bas* **1975**, 94, 112–114.

(35) GAUSSIAN 94, Revision B.2; Frisch, M. J.; Trucks, G. W.; Schlegel, H. B.; Gill, P. M. W.; Johnson, B. G.; Robb, M. A.; Cheeseman, J. R.; Keith, T.; Petersson, G. A.; Montgomery, J. A.; Raghavachari, K.; Al-Laham, M. A.; Zakrzewski, V. G.; Ortiz, J. V.; Foresman, J. B.; Cioslowski, J.; Stefanov, B. B.; Nanayakkara, A.; Challacombe, M.; Peng, C. Y.; Ayala, P. Y.; Chen, W.; Wong, M. W.; Andres, J. L.; Replogle, E. S.; Gomperts, R.; Martin, R. L.; Fox, D. J.; Binkley, J. S.; Defrees, D. J.; Baker, J.; Stewart, J. P.; Head-Gordon, M.; Gonzalez, C.; Pople, J. A. GAUSSIAN, Inc.: Pittsburgh, PA, 1995.

(36) MP2(FC) (FC = frozen core): Møller, C.; Plesset, M. S. *Phys. Rev.* **1934**, 46, 618–622. Pople, J. A.; Krishnan, R.; Schlegel, H. B.; Binkley, J. S. *Int. J. Quantum. Chem. Symp.* **1979**, 13, 225–241.

(37) Wachters, A. J. H. *J. Chem. Phys.* **1970**, 52, 1033–1036.

(38) Hay, P. J. *J. Chem. Phys.* **1977**, 66, 4377–4384.

(39) Hehre, W. J.; Radom, L.; von Ragué Schleyer, P.; Pople, J. A. *Ab Initio Molecular Orbital Theory*; John Wiley: New York, 1986; references cited therein.

(40) Fukui, K. *Acc. Chem. Res.* **1981**, 14, 363–368. Gonzalez, C.; Schlegel, H. B. *J. Chem. Phys.* **1989**, 90, 2154–2161.

transition structure (TS) at the MP2/631WH level. The *s* value refers to the reaction coordinate⁴¹ in unit of amu^{1/2}·bohr, with its zero taken at TS.

On the basis of the knowledge on the reaction pathway obtained at the MP2 level, the less-computer intensive hybrid DF method was examined to find that it is of comparable performance for the reaction of Me₂CuLi·LiCl (see Appendix).⁴² Thus, for all reagents examined here (MeCu, Me₂Cu⁻, Me₂CuLi, Me₂CuLi·LiCl, and (Me₂CuLi)₂),⁴³ geometry optimization was performed by density functional/Hartree–Fock hybrid method using the Becke's three-parameter exchange functional⁴⁴ plus Lee–Yang–Parr nonlocal correlation functional (B3LYP)⁴⁵ with the Ahlrichs "SVP" all-electron basis set⁴⁶ for copper and 6-31G(d) for the rest (denoted as B3LYP/631A), where the Ahlrichs "SVP" basis set is smaller than the Wachters + Hay set above.

Energies of the reactants, complex, and TS in the MeCu, Me₂Cu⁻, and Me₂CuLi·LiCl additions were evaluated at the MP3, MP4SDQ,⁴⁷ and CCSD(T)⁴⁸ levels. For CCSD(T) calculations of complex and TS in the Me₂CuLi·LiCl reaction, we used Ahlrichs "SVP" set for Cu and 3-21G sets for other atoms (denoted as 321A).

Relativistic effects of copper atom was examined for the reaction of Me₂CuLi·LiCl by using the B3LYP functional with a quasirelativistic pseudopotential representing 10-core electrons in conjunction with (311111/22111/411) contracted basis set developed by Dolg *et al.*⁴⁹ for copper and 6-31G(d) basis sets for the rest (denoted as B3LYP/631D).

Stationary points were optimized without any symmetry assumption unless noted otherwise. All TSs and symmetry-constraint stationary points obtained with the 631WH and 631A basis were characterized by normal coordinate analysis at the same level of theory (number of imaginary frequency = 0 for minima and 1 for TSs). Natural charges⁵⁰ are calculated at the same level as the level for geometry optimizations.

The Boys localization procedure⁵¹ was performed to obtain localized MOs from the occupied B3LYP/631A Kohn–Sham MOs⁵² for MP2/631WH geometries. The total electron density is not changed by this transformation.

Comparison of Theoretical Methods. In numerous previous studies on organocopper reactions, various theoretical methods have been employed largely without systematic evaluation of their performance. Until recently, the *ab initio* MP2 level calculations have been accepted as the best available method for organocopper chemistry, yet density functional (DF) methods have emerged recently as methods of higher cost performance. However, the reliability of the DF method in the analysis of dynamic behavior of organocopper reagents has not yet been proven. In the present studies, we have systematically examined the performance of the DF method against standard *ab initio* methods of established general reliability.

We initially performed a series of calculations on the reaction of Me₂CuLi·LiCl with acetylene at the RMP2(FC)/631WH level (struc-

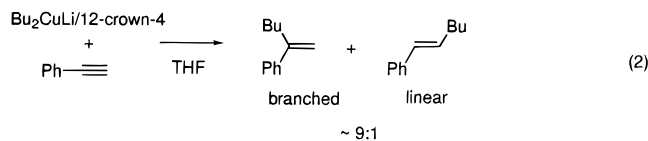
tures and energies summarized in Figure 8A). Then, we reexamined the same reaction at the B3LYP/631A level to find that the structures of the stationary points are very similar to the MP2 ones (Figure 8B). Good agreement with the experimental structural data was for various theoretical levels (see Appendix).

Further comparison of the energies at the MP2 and B3LYP levels was made against the MP3, MP4SDQ, and CCSD(T) level calculations based on the B3LYP/631A geometries, for the reaction of acetylene with MeCu, Me₂Cu⁻, and Me₂CuLi·LiCl. The detailed numbers are shown in Figure 12 and Appendix. The data indicate that the B3LYP values are closer to the CCSD(T) values than the MP2 values are. The activation energies are quite different between the MP2 and the B3LYP methods.

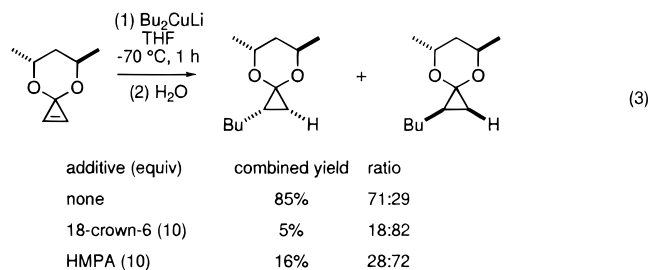
As examined for the reaction of Me₂CuLi·LiCl (Figure 8B vs 8C), the relativistic effects (B3LYP/631A vs B3LYP/631D) on the structures of complex and TS and the activation energies were found to be very small (maximum 1.7% geometry difference). Further details of the comparison is given later in the Appendix.

Results

Experiments. In order to obtain experimental data on the role of lithium counterion in carbocupration chemistry, a series of experiments on the effect of added crown ether were performed. Parallel experiments have already been reported for the conjugate addition.⁴ Phenylacetylene reacts smoothly with 1 equiv of Bu₂CuLi·LiI at -40 °C for 4 h to give a 91:9 mixture of a branched and a linear adduct, respectively, in 56% combined yield. When the same reaction was carried out in the presence of 10 equiv of 12-crown-4, the reaction slowed down considerably (12% under the same conditions) and completed only after 18 h at -20 to 0 °C (53% yield; 85:15



isomer distribution). In similar experiments using a cyclopropanone acetal (eq 3), the carbocupration with Bu₂CuLi·LiBr·Me₂S took place very slowly in the presence of HMPA or 18-crown-6 and did not lead to completion under conditions where Bu₂CuLi·LiBr·Me₂S itself reacted quickly.⁵³ The change of the diastereoselectivity suggests that the reactive species may change upon addition of the solvating agents. Thus, it was found that a crown ether slows down the carbocupration reaction as well as conjugate addition and acylation reactions, which have been reported previously.⁴



Cuprate Models. Structures of Me₂Cu⁻ (linear) and R₂CuLi dimers (A) known from crystallographic studies^{10,54} suggest that the cuprate R–Cu–R structure prefers a linear arrangement. In fact, we found that bending of the linear Me–Cu–Me

(53) Isaka, M. Ph.D. Dissertation, Tokyo Institute of Technology, Chapter 3, 1991; pp 83–84.

(54) Hope, H.; Olmstead, M. M.; Power, P. P.; Sandell, J.; Xu, X. *J. Am. Chem. Soc.* **1985**, *107*, 4337–4338.

(41) Gonzalez, C.; Schlegel, H. B. *J. Phys. Chem.* **1990**, *94*, 5523–5527.

(42) At the other basis sets with B3LYP and MP2 methods. See: (a) Snyder, J. P.; Bertz, S. H. *J. Org. Chem.* **1995**, *60*, 4312–4313. (b) Cui, Q.; MUSAEV, D. G.; Svensson, M.; Morokuma, K. *J. Phys. Chem.* **1996**, *100*, 10936–10944. (c) Hertwig, R. H.; Koch, W.; Schröder, D.; Schwarz, H.; Hrušák, J.; Schwerdtfeger, P. *J. Phys. Chem.* **1996**, *100*, 12253–12260. (d) Barone, V. *J. Phys. Chem.* **1995**, *99*, 11659–11666.

(43) Böhme, M.; Frenking, G.; Reetz, M. T. *Organometallics* **1994**, *13*, 4237–4245.

(44) Becke, A. D. *J. Chem. Phys.* **1993**, *98*, 5648–5652.

(45) Lee, C.; Yang, W.; Parr, R. G. *Phys. Rev. B* **1988**, *37*, 785–789.

(46) Schäfer, A.; Horn, H.; Ahlrichs, R. *J. Chem. Phys.* **1992**, *97*, 2571–2577.

(47) Trucks, G. W.; Salter, E. A.; Sosa, C.; Bartlett, R. J. *Chem. Phys. Lett.* **1988**, *147*, 359–366.

(48) Scuseria, G. E.; Scheiner, A. C.; Lee, T. J.; Rice, J. E.; Schaefer III, H. F. *J. Chem. Phys.* **1987**, *86*, 2881–2890. Pople, J. A.; Head-Gordon, M.; Raghavachari, K. *J. Chem. Phys.* **1987**, *87*, 5968–5975.

(49) Dolg, M.; Wedig, U.; Stoll, H.; Preuss, H. *J. Chem. Phys.* **1987**, *86*, 866–872.

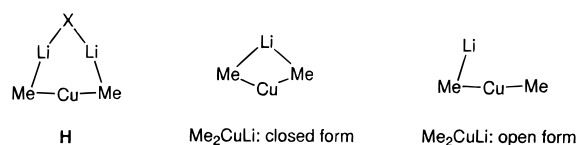
(50) Reed, A. E.; Curtiss, L. A.; Weinhold, F. *Chem. Rev.* **1988**, *88*, 899–926. NBO Version 3.1 in Gaussian 94 package; implemented by Glendening, E. D.; Reed, A. E.; Carpenter, J. E.; Weinhold, F.

(51) Boys, S. F. *Quantum Theory of Atoms, Molecules, and the Solid State*; Lowdin, P. O., Ed.; Academic Press: New York, 1968; pp 253–262. Haddon, R. C.; Williams, G. R. *J. Chem. Phys. Lett.* **1976**, *42*, 453–455.

(52) Kohn, W.; Sham, L. *J. Phys. Rev.* **1965**, *140*, A1133–A1138.

structure in free Me–Cu–Me anion to $\angle\text{C–Cu–C} = 116^\circ$ (the angle found in the $\text{Me}_2\text{CuLi}/\text{acetylene}$ complex later in Figure 5) results in as much as 28.0 kcal/mol increase of energy (B3LYP/631A//B3LYP/631A). Theoretical studies by Snyder and Frenking on various possibilities of cuprate structures not only reproduced the pertinent properties of the crystallographic structures^{10,11,43,54,55} but also led to proposals of some others, such as **H**. The geometries of our cuprate models are based on these experimental and theoretical studies.

For the structure of the smallest lithium organocuprate cluster Me_2CuLi , an open and a C_{2v} closed form (see below) have been considered.⁴³ With the Me–Cu–Me moiety being bent and strained, the closed structure is not even a local minimum. Though the Me–Cu–Me group is in its favorable linear geometry in the open form (as shown later in Figure 5), the positive charges in the coordination-free Li atom and the negative charge in one of the two methyl groups are placed far away from each other and cannot enjoy favorable charge interaction.⁵⁶ As a consequence, the Me_2CuLi cluster is less stable than its symmetrical dimer (**A**, $\text{R} = \text{Me}$).⁴³ One may postulate that the Me_2CuLi minimum cluster exists in a very polar basic solvent. The consequence of such solvation will be either the attenuation of the Lewis acidity of the lithium atom or the formation of naked Me_2Cu^- as experimentally shown for the case of crown ether solvation (vide supra).⁵⁴



Especially noteworthy is the recent proposal of a six-centered monomeric cuprate **H** for $\text{X} = \text{Me}$, CN , and I .^{11,55} The structure of $\text{Me}_2\text{CuLi}\cdot\text{LiCl}$ cluster can be viewed as a composite of half of the eight-centered structure **A** and half of a four-centered lithium halide dimer.⁵⁷ Both have been supported by crystallography, and, hence, **H** appears to be a reasonable structure. Although structures **A** and **H** differ in their numbers of copper atoms (i.e., dimer vs monomer), they exhibit close similarity for the Li–R–Cu–R–Li moiety (for details see Figures 9 and 10, Table 1). In view of this similarity, we conjectured that the monomer **H** will serve as a good model for studies of the dimer cluster **A**, if the remaining part (i.e., the upper part) of the molecule in **A** and **H** does not actively take part in the cuprate reaction. As will be reported below, this assumption was found to be reasonable. This assumption was also practically important prior to our finding that B3LYP method performs very well in the studies on cuprate chemistry^{42a,55} (vide supra), since the current level of computational power does not allow extensive studies on the dimer possessing two copper atoms at the *ab initio* level better than that of the MP2 method. We found this level to be the minimum level of the *ab initio* calculations for the studies on cuprate reactions. From the chemical point of view, it must be noted that studies using a

(55) (a) Snyder, J. P.; Tipsword, G. E.; Splanger, D. J. *J. Am. Chem. Soc.* **1992**, *114*, 1507–1510. (b) Snyder, J. P.; Splanger, D. P.; Behling, J. R.; Rossiter, B. E.; *J. Org. Chem.* **1994**, *59*, 2665–2667. Stemmler, T. L.; Barnhart, T. M.; Penner-Hahn, J. E.; Tucker, C. E.; Knochel, P.; Böhme, M.; Frenking, G. *J. Am. Chem. Soc.* **1995**, *117*, 12489–12497. Huang, H.; Alvarez, K.; Cui, Q.; Barnhart, T. M.; Snyder, J. P.; Penner-Hahn, J. E. *J. Am. Chem. Soc.* **1996**, *118*, 8808–8816, and **1996**, *118*, 12252 (correction).

(56) Lambert, C.; von Ragué Schleyer, P. *Angew. Chem., Int. Ed. Engl.* **1994**, *33*, 1129–1140.

(57) Hall, S. R.; Raston, C. L.; Skelton, B. W.; White, A. H. *Inorg. Chem.* **1983**, *22*, 4070–4073. Amstutz, R.; Dunitz, J. D.; Laube, T.; Schweizer, W. B.; Seebach, D. *Chem. Ber.* **1986**, *119*, 434–443. Raston, C. L.; Whitaker, C. R.; White, A. H. *Aust. J. Chem.* **1989**, *42*, 201–207.

Table 1. Comparison of Theoretical Methods for Representative Structural Parameters of **RT1-d** [$\text{R} = \text{Me}$: (Me_2CuLi)₂] and **RT1w** [$\text{R} = \text{Me}$: ($\text{Me}_2\text{CuLi}(\text{OH}_2)$)₂] and **RT1** (**H**, $\text{X} = \text{Cl}$: $\text{Me}_2\text{CuLi}\cdot\text{LiCl}$)

model	level	C–Cu ^a	C–Li ^a	C–Cu–C ^b
RT1-d	B3LYP/631A	1.991	2.070	171.3
	MP2/631HW ^c	1.968	2.043	174.2
RT1w	B3LYP/321A	1.987	2.229, 2.207	168.4
	MP2/321HW ^c	1.983	2.259, 2.240	168.5
RT1	HF/631WH	2.066	2.071	177.4
	B3LYP/631A	1.994	2.087	177.9
	MP2/631WH	1.948	2.140	174.4

^a Bond lengths in Å. ^b Angles in deg. ^c Reference 43.

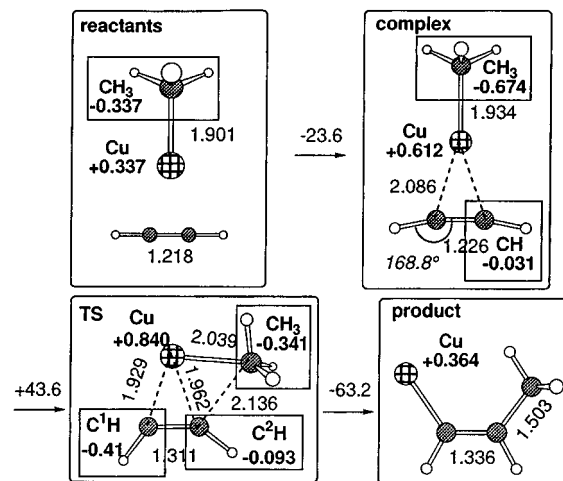


Figure 1. Stationary points of the MeCu addition to acetylene. MeCu , acetylene, complex, TS, and product were optimized with C_{3v} , $D_{\infty h}$, C_{2v} , C_s , and C_s symmetries, respectively. Bond lengths and angles at the B3LYP/631A are shown in Å and deg, respectively. Energy changes at the B3LYP/631A//B3LYP/631A level are shown on the arrows in kcal/mol. The value of imaginary frequency at TS is $494.7i \text{ cm}^{-1}$. Natural charges on atoms or groups in boxes are in bold. Total energies of MeCu and acetylene are -1680.21688 and -77.32565 hartrees at the B3LYP//B3LYP/631A level, respectively.

monomer model such as Me_2CuLi and $\text{Me}_2\text{CuLi}\cdot\text{LiCl}$ are no less important than those using a dimer, as monomer participation is also widely considered as one possibility (although it is not clearly supported nor eliminated by experiments).

Therefore, we selected the Snyder model **H** with $\text{X} = \text{Cl}$ as the first model of lithium organocuprate cluster^{11,55} and examined the stationary points in the acetylene reaction and the structures on the IRC of the carbocupration reaction by the MP2/631WH method. Such a careful structure search was necessary owing partly to the lack of precedent on the dynamic studies of cuprate clusters and partly to the structural and electronic complexity of the system under consideration. With detailed information on the reaction of $\text{Me}_2\text{CuLi}\cdot\text{LiCl}$ at the MP2 level, we then found that the B3LYP method is reliable enough and used it for all other reactions. As shown below, comparison of $\text{Me}_2\text{CuLi}\cdot\text{LiCl}$ and dimer indicated that the essence of the cuprate cluster reactivities do reside in the Li–Me–Cu–Me–Li part structure of the cluster. The same was found in the conjugate addition reaction reported in the following article.²⁶

MeCu Addition. We first examined the simplest model, the MeCu addition to acetylene, with the B3LYP/631A method (Figures 1 and 2), and located a π -complex, a TS, and a product. The geometries and energies are very similar to the Hartree–Fock results reported previously.⁵⁸ The complex formation takes place with a very large stabilization energy (23.6 kcal/mol, B3LYP/631A//B3LYP/631A), and the activation energy of C–C bond formation was also very high (43.6 kcal/mol, B3LYP/

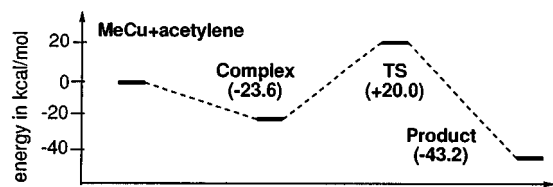


Figure 2. Energy profile in the MeCu addition to acetylene. Energies relative to reactants (B3LYP/631A//B3LYP/631A) in kcal/mol are shown in parentheses.

631A//B3LYP/631A). In the complex, there are only small changes in structure (and charge) for the acetylene moiety, as found for the crystal structure of acetylene complexes of Lewis acidic CuX (X = Cl, etc.) salt⁵⁹ and for the previously calculated structure of $[\text{Cu}(\text{C}_2\text{H}_2)]^+$.⁶⁰ The MeCu/acetylene complexation is a simple electrostatic complex in its character, with the substantial dipole of $\text{Cu}^{+\delta}\text{Me}^{-\delta}$ interacting with the π -electron cloud of acetylene which further polarizes CuMe. The addition reaction may be best viewed as a simple four-centered addition reaction (namely, the metal acting as a Lewis acid) as previously reported.^{32,58} The high calculated activation energy is consistent with the fact that alkylcopper compounds alone are not (experimentally) reactive nucleophilic reagents.

Me₂Cu⁻ Addition.⁶¹ Interaction of Me₂Cu⁻ with acetylene (Figures 3 and 4) affords a complex with 0.8 kcal/mol stabilization energy (B3LYP/631A//B3LYP/631A). Though the stabilization energy is much smaller than that obtained for MeCu, the structure of the complex indicates tighter binding between the cuprate and the acetylene (cf. the longer C¹–C² and the shorter C¹–Cu bond lengths as well as the acetylene deformation), and a significant amount of negative charge is transferred to acetylene. Since linear Me₂Cu⁻ has no permanent dipole, the electrostatic interaction is small as reflected in the small stabilization energy. The interaction comes mainly from the Me₂Cu⁻ HOMO-2 (mainly corresponding to Cu 3*d* orbital)–acetylene LUMO charge transfer interaction. The *sp*-hybridized acetylene acts a good electron acceptor. The structure of the complex and TS are very similar to the Me₂Cu⁻/acetylene part structure in the π -complexes of Me₂CuLi, Me₂CuLi·LiCl, and (Me₂CuLi)₂ (vide infra). The activation energy of 20.3 kcal/mol (B3LYP/631A//B3LYP/631A) is still high, though it is much lower than that found for MeCu. This is consistent with the low reactivity of the crown-solvated cuprate reagents.

Me₂CuLi Addition. In the reaction of the minimum cluster Me₂CuLi (Figures 5 and 6), the open cluster closes upon complexation with acetylene as the linear Me–Cu–Me bond is bent by complexation. The cluster closing causes the lithium cation to be stabilized by the two negatively charged methyl groups and therefore results in stabilization of the complex by as much as 17.8 kcal/mol (B3LYP/631A//B3LYP/631A). Such a large stabilization is reflection of the instability of the Me₂CuLi monomer and is not observed in larger clusters (vide infra), wherein all negative and positive charges are electrostatically

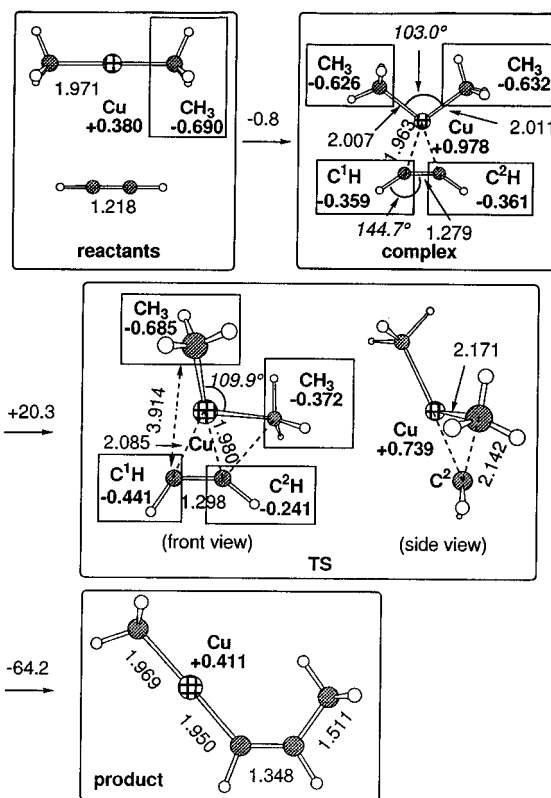


Figure 3. Stationary points of the Me₂Cu⁻ addition to acetylene. Me₂Cu⁻, acetylene, complex, and product were optimized with *D*_{3h}, *D*_{∞h}, *C*_s, and *C*_s symmetries, respectively. TS was optimized with no symmetry. Bond lengths and angles at the B3LYP/631A are shown in Å and deg, respectively. Energy changes at the B3LYP/631A//B3LYP/631A level are shown on the arrows in kcal/mol. The value of imaginary frequency at TS is 392.8i cm⁻¹. Natural charges on atoms or groups in boxes are in bold. In the TS described in this and Figures 5, 8, and 13, the front views place C¹–C²–H or the plane of the paper, the side view places C¹–C²–H perpendicular to the plane. Total energies of Me₂Cu⁻ and acetylene are –1720.163 36 and –77.325 645 hartrees at the B3LYP/631A//B3LYP/631A level, respectively.

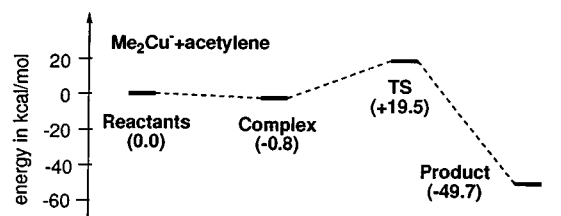


Figure 4. Energy profile in the Me₂Cu⁻ addition to acetylene. Energies relative to reactants (B3LYP/631A//B3LYP/631A) in kcal/mol are shown in parentheses.

stabilized already in the starting clusters. The negative charge developing on an acetylenic carbon terminus is now stabilized by the lithium cation inside the cluster structure, and the activation energy decreases to 15.8 kcal/mol. The charge stabilization by the lithium atom causes the deformation of the TS of Me₂Cu⁻ addition (Figure 5), changing the Me–Cu–Me angle from 109.9° to 141.3° and lengthening the Cu–CH bond (2.250 Å). The activation energy of 15.8 kcal/mol is lower than that of Me₂Cu⁻, comparable with that of (Me₂CuLi)₂, and higher than that of Me₂CuLi·LiCl (vide infra). The C³–Cu–C⁴ bond angle is much wider (141°) than those in others, which are consistently between 109° and 126°.

Me₂CuLi·LiCl Addition

1. MP2 Studies. From the HF studies described in the Appendix, it became clear that the calculations on the cuprate

(58) Nakamura, E.; Miyachi, Y.; Koga, N.; Morokuma, K. *J. Am. Chem. Soc.* **1992**, *114*, 6686–6692. Nakamura, E.; Nakamura, M.; Miyachi, Y.; Koga, N.; Morokuma, K. *J. Am. Chem. Soc.* **1993**, *115*, 99–106.

(59) (a) Thompson, J. S.; Whitney, J. F. *J. Am. Chem. Soc.* **1983**, *105*, 5488–5490. (b) Munakata, M.; Kitagawa, S.; Kawada, I.; Maekawa, M.; Shimono, H. *J. Chem. Soc., Dalton Trans.* **1992**, 2225–2230. (c) Brantin, K.; Håkansson, M.; Jagner, S. *J. Organomet. Chem.* **1994**, *474*, 229–236.

(60) Böhme, M.; Wagener, T.; Frenking, G. *J. Organomet. Chem.* **1996**, *520*, 31–43.

(61) In the Me₂Cu⁻ addition to acetylene, the geometries of complex and TS as well as the activation energy were found to be unaffected (<1.2% for geometry and 0.3 kcal/mol for energy) by addition of a diffuse *sp* function of exponent $\alpha = 0.438$ for carbon (Clark, T.; Chandrasekhar, J.; Spitznagel, G. W.; von Ragué Schleyer, P. J. *Comput. Chem.* **1983**, *4*, 294–301).

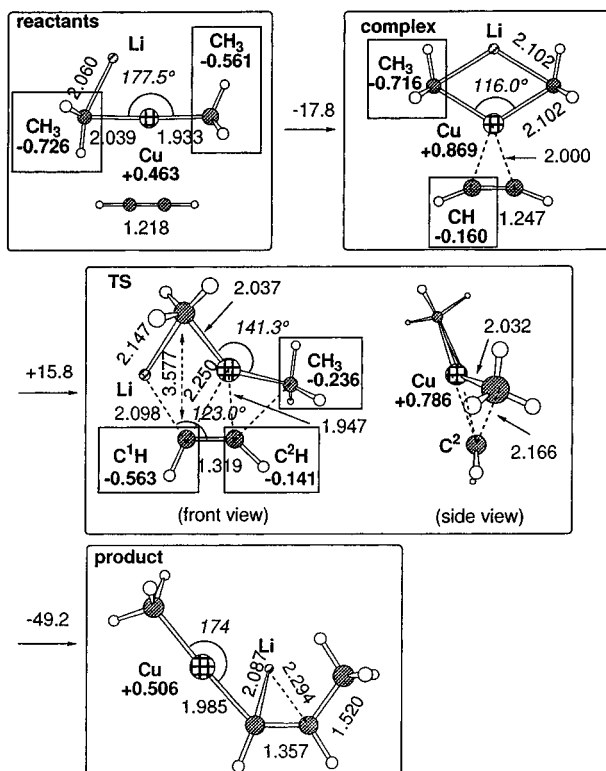


Figure 5. Stationary points of the Me_2CuLi addition to acetylene. Me_2CuLi , acetylene, and complex were optimized with C_s , $D_{\infty h}$, and C_{2v} symmetry, respectively, and others with no symmetry. Bond lengths (and bond angles) at the B3LYP/631A level are shown in angstroms and degrees, respectively. The value of imaginary frequency of TS is $297.2i \text{ cm}^{-1}$. Natural charges on atoms or groups in boxes are in bold. Energies of Me_2CuLi and acetylene are -1727.687180 and -77.325645 hartrees at the B3LYP/631A/B3LYP/631A level, respectively.

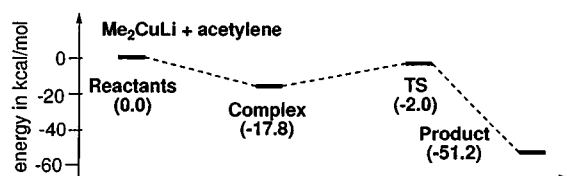


Figure 6. Energy profile in the Me_2CuLi addition to acetylene. Energies relative to reactants (B3LYP/631A/B3LYP/631A) in kcal/mol are shown in parentheses.

cluster mandate consideration of dynamical electron correlation effects. The importance in the treatment of these effects is also in consonance with what is generally agreed for *ab initio* calculations on first row transition metals.⁶² Thus we studied MP2 calculations of $\text{Me}_2\text{CuLi}\cdot\text{LiCl}$ addition to acetylene. First with the MP2 method and then with the B3LYP method, both of which led to the same chemical conclusion.

Figure 7 shows the energies and other parameters for the structures of the stationary points on the potential surface as obtained by MP2 optimization.⁶³ A summary of the findings that will be detailed below is schematized as a five-phase scheme, a trap-and-bite mechanism (Scheme 4, X = Cl and also for $\text{Me}-\text{Cu}-\text{Me}$ (vide infra)). The net process constitutes the conversion of one six-centered cuprate (**RT1**) to another (**PD**). The above pathway may be viewed as *copper-assisted*

(62) Lüthli, H. P.; Siegbahn, P. E. M.; Almlöf, J. *J. Phys. Chem.* **1985**, *89*, 2156–2161. Siegbahn, P. E. M.; Svensson, M. *Chem. Phys. Lett.* **1993**, *216*, 147–154.

(63) We obtained for the pathway between **INT1** and **INT2** as shown in Figures 7 and 8A by IRC analysis at the MP2/631WH level. **INT1** and **INT2** are nonstationary points and **INT1** and **INT2** led to **CP** and **PD** with the minimum search, respectively.

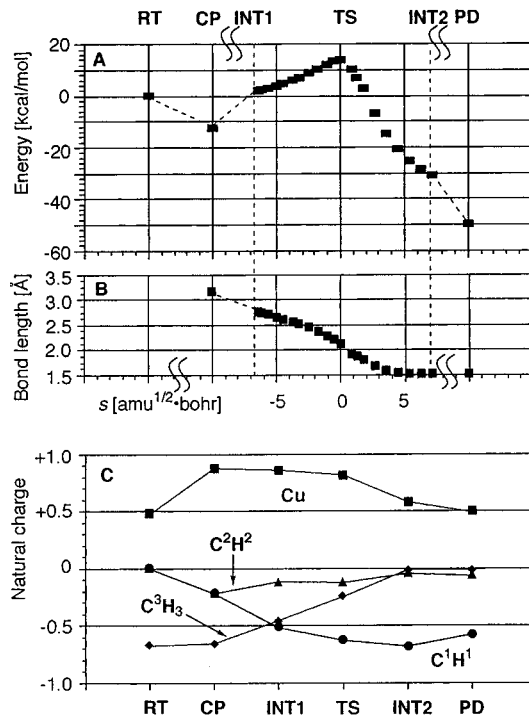
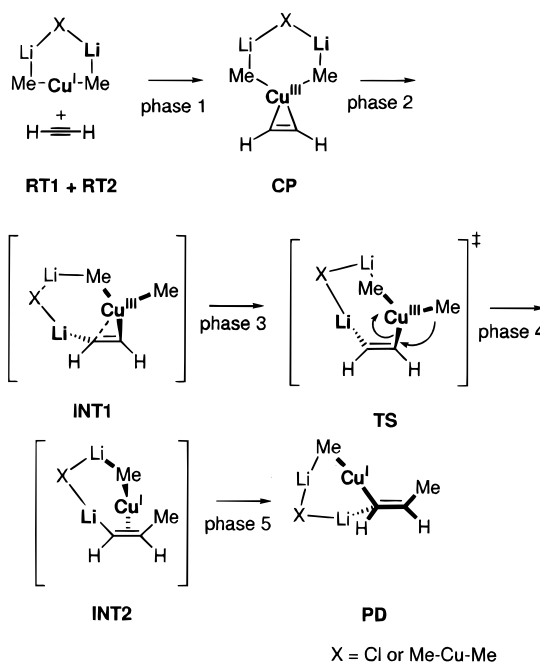


Figure 7. Structures, energies, and charges in the addition of $\text{Me}_2\text{CuLi}\cdot\text{LiCl}$ to acetylene. (A) Energy relative to reactants, (B) C^2-C^3 bond length, and (C) natural charges for various points on the reaction pathway as obtained at the MP2/631WH/MP2/631WH level. The pathway between **INT1** and **INT2** was obtained by following the IRC down from **TS**. Structural correlation between **CP** and **INT1** as well as between **INT2** and **PD** was confirmed by usual optimization procedure.

Scheme 4. Trap-and-Bite Mechanism for the Addition of Organocuprate to Acetylene



carbolithiation followed by intracuster transmetalation. In the first phase of the reaction (phase 1), the cluster traps acetylene with its copper atom to form **CP**. Negative charge flows from Cu(I) to acetylene (Figure 7C) to liberate the C^3 methyl group free from coordination to Li^1 (phase 2). **INT1** is an example of the structure connecting **CP** and **TS**. Though this process involves a major bond reorganization, such a process involving the cleavage of a dicoordinated lithium atom and a pentacoor-

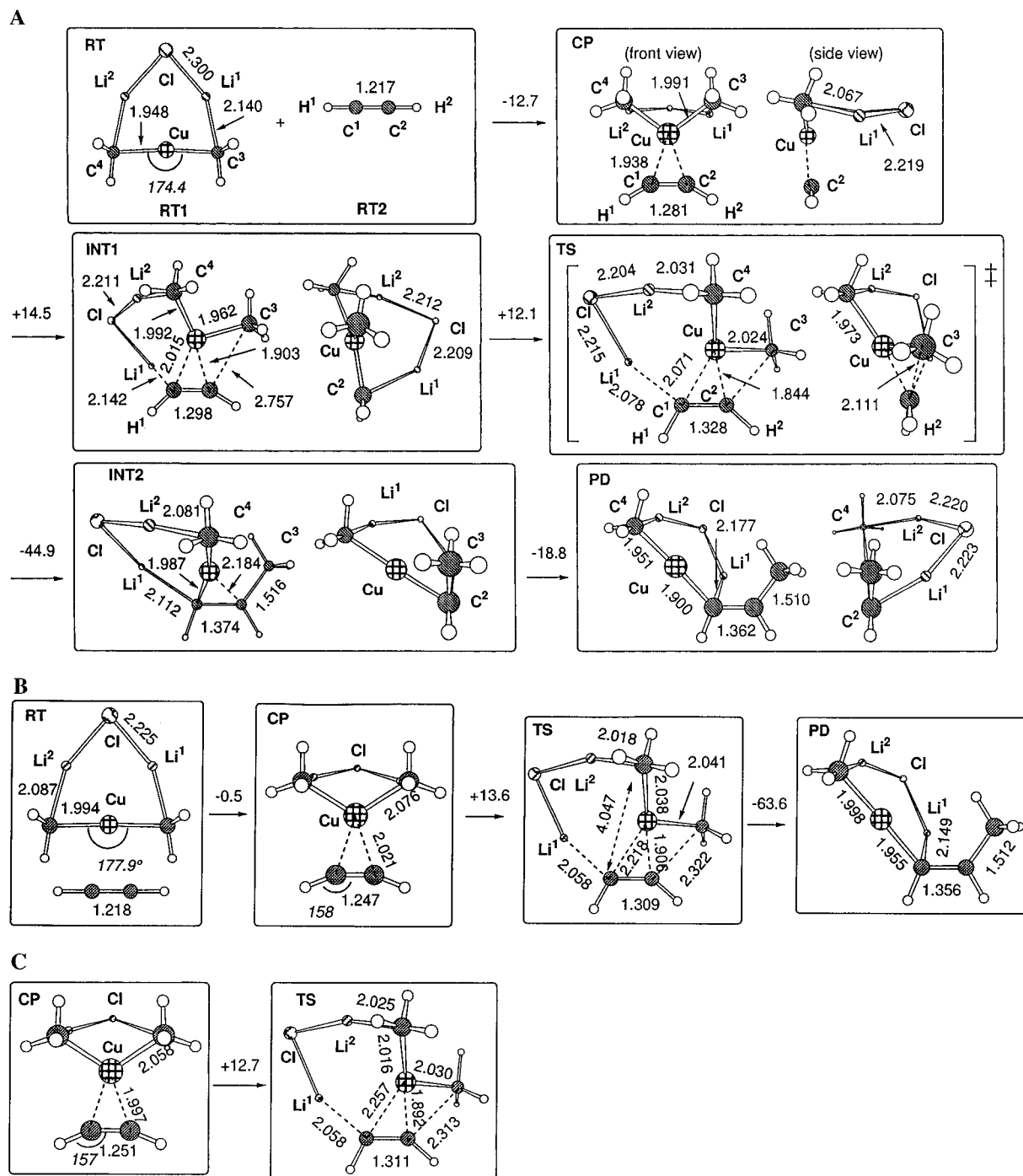


Figure 8. (A) Complexes, TS, and representative structures in the reaction of $\text{Me}_2\text{CuLi}\cdot\text{LiCl}$ with acetylene obtained at the MP2/631WH level. Bond lengths and angles are shown in Å and deg, respectively. Energy changes at the MP2/631WH/MP2/631WH level are shown on the arrows in kcal/mol. **INT1** is a structure at $s = -6.41 \text{ amu}\cdot\text{bohr}^{-1/2}$ from **CP** to **TS** and **INT2** is a structure at $s = +7.18 \text{ amu}\cdot\text{bohr}^{-1/2}$ from **TS** to **PD** on the reaction path. The value of imaginary frequency of **TS** is $391.7i \text{ cm}^{-1}$. The total energies of **RT1** and **RT2** are -2193.38313 and -77.06679 hartrees, respectively. (B) Stationary points in the $\text{Me}_2\text{CuLi}\cdot\text{LiCl}$ addition to acetylene obtained at the B3LYP/631A level. The value of imaginary frequency of **TS** is $191.38i \text{ cm}^{-1}$. (C) Complex and TS in the $\text{Me}_2\text{CuLi}\cdot\text{LiCl}$ addition to acetylene obtained at the B3LYP/631D level, which takes into account relativistic effects on copper.

minated methyl group in solution is expected to be a very low energy process as is known for the behavior of alkyl lithium clusters in ethereal solution.⁶⁴ By the transformation through a series of structures (**INT1** to **INT2**), the open cluster bites into the substrate (phases 3 and 4). It is at this stage that new C–C and C–Li bonds are formed at the expense of a covalent C–Cu bond. After propenyllithium formation (cf. **INT2**, a nonstationary point), intramolecular transmetalation from Li to

Cu (phase 5) makes the energy drop further to produce the propenylcopper product (**PD**).

The representative 3D-structures on the reaction pathway of the $\text{Me}_2\text{CuLi}\cdot\text{LiCl}$ reaction are shown in Figure 8 and energies in Figure 9. Interaction of **RT1** with **RT2** bends the linear $\text{C}^3\text{—Cu—C}^4$ bonding to form a complex (**CP**, near C_s symmetry) (Figure 7A and 8A).⁶⁵ $\text{C}^1\text{—C}^2\text{—Cu—C}^4$ dihedral angle of 166.5° indicates nearly square planar geometry consistent with d^8 Cu(III) formalism.^{19,20} The conversion from **RT1** to **CP** accompanied with a change (though small) of d -orbital population

(64) Cf.: McGarrity, J. F.; Ogle, C. A.; Brich, Z.; Loosli, H.-R. *J. Am. Chem. Soc.* **1985**, *107*, 1810–1815.

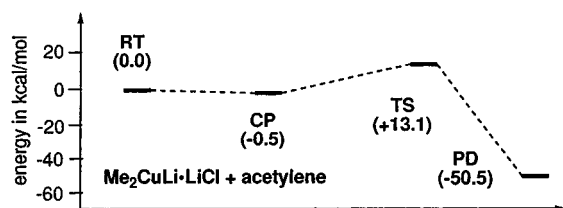


Figure 9. Energy profile in the $\text{Me}_2\text{CuLi}^+\text{LiCl}$ addition to acetylene. Energies relative to reactants (B3LYP/631A//B3LYP/631A) in kcal/mol are shown in parentheses.

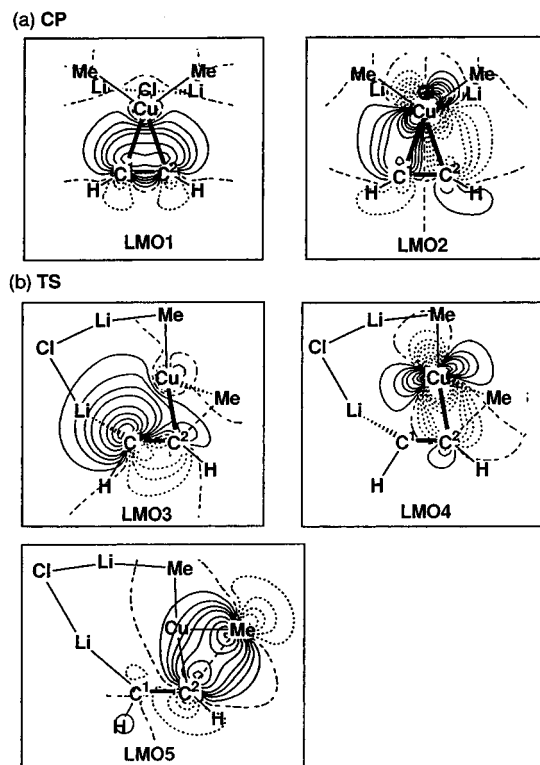


Figure 10. Contour plots of localized Kohn-Sham MOs (B3LYP/631A//MP2/631WH) of (a) CP and (b) TS in the $\text{C}^1\text{-C}^2\text{-Cu}$ (LMO1-4) and the $\text{C}^2\text{-C}^3\text{-C}^4$ (LMO5) planes. Contour levels in $e\text{-au}^{-3}$ are from -0.30 to $+0.30$ at intervals of 0.05 . Positive contours are solid, negative dotted, and nodal lines dashed.

[$4s(0.74)$, $3d(9.64)$ in **RT1** and $4s(0.52)$, $3d(9.46)$ in **CP**] in natural charge (MP2) suggested the presence of backdonation from Cu to acetylene. The typical donation-backdonation interaction^{33,66} is clearly seen in the occupied localized Kohn-Sham MOs in Figure 10 (donation in **LMO1** and back-donation in **LMO2**), and hence the complex should be better viewed as a cupriocyclopropene rather than a simple π -donation complex.⁶⁷

For a reaction of such complexity, information from stationary points (**CP**, **TS**, and **PD**) was not enough to understand the reaction pathway. We therefore studied the structures along the MP2-IRC to find that important intracluster transformations are taking place between the stationary points. Thus, by following the down-energy IRC from **TS** toward **CP** (Figure 7A), we reached **INT1** (a nonstationary point, Figure 8A), which is an example of an intermediary structure connecting **CP** and

(65) **CP** at the RMP2(FC) geometry showed slight triplet instability of RHF wave function (the expectation value of S^2 was however only 0.052 in the UHF calculation). RB3LYP/631A wave functions for both **CP** and **CP-d** at the RB3LYP geometries were found to be stable. See: Seeger, R.; Pople, J. A. *J. Chem. Phys.* **1977**, *66*, 3045-3050.

(66) Dewar, M. J. S. *Bull. Chim. Soc. Fr.* **1951**, C71-C77. Chatt, J.; Duncanson, L. A. *J. Chem. Soc.* **1953**, 2939-2947.

(67) No cuprate/acetylene complex could be located on the potential surface of the HF/631WH level calculations.

Table 2. Comparison of Activation Energies (**TS** - **CP**) in kcal/mol for Various Levels of Theoretical Methods at the MP2/631WH Optimized Geometries of **CP** and **TS**

method/basis set	321A	631WH
MP2		26.6
MP3	14.4	14.4
MP4DQ	18.2	21.3
MP4SDQ	16.2	19.9
CCSD(T)	15.4	
B3LYP ^a	12.6	13.6

^a Geometry optimization performed at the same level.

TS. Note that, with the usual geometry optimization procedure, **INT1** further goes down hill to **CP** with smooth migration of Li^1 to C^3 .

In **INT1**, the $\text{C}^3\text{-Li}^1$ bond is completely cleaved (4.278 \AA) and Li^1 is coordinated to the π -orbital of C^1 (negatively charged, Figure 7C) perpendicular to the $\text{C}^1\text{-C}^2\text{-H}^2$ plane. $\text{Li}^1\text{-C}^1\text{-C}^2\text{-H}^2$ dihedral angle is -116° . In **TS**, the free C^3 anion will undergo C-C bond formation with C^2 . Further along the reaction path toward **TS**, cleavage of $\text{C}^3\text{-Cu}$ bond results in an increase and decrease of negative charge on C^1H^1 and C^3H_3 , respectively (Figure 7C).

In **TS**, a few important events are taking place simultaneously. One is the rapid formation of $\text{C}^2\text{-C}^3$ bond (Figure 7B) with retention of the planar coordination geometry of Cu (Figure 8).⁶⁸ The LMO in Figure 10 (**LMO5**) illustrates $\text{C}^2\text{-C}^3$ bond formation. The relatively short Cu-C^2 bond (1.844 \AA) is noteworthy and is formed mainly by the copper's filled $3d$ orbitals as shown in **LMO4** in Figure 10. The second notable geometry change is that Li^1 is forming a σ -bond with C^1 . **LMO3** in Figure 10 indicates that the C^2 's filled sp^n orbital strongly interacts with Li^1 as well as with Cu^1 . According to a recent proposal,⁶⁹ the C^1 atom can be considered to act as a donor ligand for a Cu(III) species. Comparison of the localized MOs in Figure 10 indicates that the molecular orbital interactions characterizing the donation/backdonation interaction in **CP** (**LMO1** and **LMO2**) changes to those characterizing Cu(III) reductive elimination (**LMO3** and **LMO4**).

The barrier height from **CP** to **TS** is 26.6 kcal/mol at the MP2/631WH//MP2/631WH level and decreases by several kcal/mol at higher levels (Table 2). The value for the best level CCSD(T)/631WH can be estimated from MP4SDQ/631WH, CCSD(T)/321A, and MP4SDQ/321A results to be 19.1 kcal/mol . The activation energy remains unaffected (MP2 level, 26.5 kcal/mol) by solvent polarity (THF, $\epsilon_0 = 7.58$, with the self-consistent reaction field method (based on Onsager model)⁷⁰ applied without structure optimization). The B3LYP studies using an explicit solvent molecule on Li^1 in the conjugate addition of $(\text{Me}_2\text{CuLi})_2$ (the following paper)²⁶ revealed that solvation effects are small. The role of the bridging Li-Cl-Li moiety was noted clearly for the **TS**. Thus, upon hypothetically removing the $\text{Li}^1\text{-Cl-Li}^2$ bridge, the activation energy increased to 33.4 kcal/mol (MP2/631WH//MP2/631WH). This value coincides with the activation energy of 36.9 kcal/mol (MP2/631WH//B3LYP/631A) obtained for free Me_2Cu^- and indicates that the charge stabilization by the Li^1 atom contributes to lower the energy barrier.

(68) RHF/631WH wave functions for **TS** at the RMP2/631WH geometries were found to be stable.

(69) Dorigo, A. E.; Wanner, J.; von Ragué Schleyer, P. *Angew. Chem., Int. Ed. Engl.* **1995**, *34*, 476-478. Snyder, J. P. *J. Am. Chem. Soc.* **1995**, *117*, 11025-11026.

(70) Onsager, L. *J. Am. Chem. Soc.* **1936**, *58*, 1486-1493. Tapia, O.; Goscinski, O. *Mol. Phys.* **1975**, *29*, 1653-1661. Wong, M. W.; Wiberg, K. B.; Frisch, M. J. *J. Chem. Phys.* **1991**, *95*, 8991-8998. Wong, M. W.; Wiberg, K. B.; Frisch, M. J. *J. Comput. Chem.* **1995**, *16*, 385-394.

In **TS**, Li^1 moves into, and Cu out of, the $\text{C}^1\text{--C}^2\text{--H}^2$ plane, altering the nature of bonding between the acetylenic carbons and the metals. This change continues until **INT2** (a nonstationary structure, Figure 7A, see also Figure 8A), where Li^1 forms a σ -bond with sp^2 -hybridized C^1 , and Cu coordinates to the carbon π -orbital perpendicular to the $\text{C}^1\text{--C}^2\text{--H}^2$ plane. This event generates propenyllithium π -complexed with CH_3Cu (**INT2**, Figure 8A). The structural changes accompany the change of Cu(III) into simple MeCu(I) , which is reflected in the decrease of the positive charge density on Cu (Figure 7C, i.e., larger in **TS**, and smaller in **INT2** and **PD**).

The propenyllithium structure **INT2** is not a local minimum, and the usual geometry optimization smoothly converted **INT2** to **PD**. The structural change represents the conversion of **INT2** to the propenylcopper π -complexed with Li via intramolecular transmetalation. The lowering of the energy after the completion of the C--C bond formation, which is found in Figure 7A, is due to the formation of covalent C--Cu bond. It is notable that, throughout the reaction, the structure of the $\text{Li}^1\text{--Cl--Li}^2$ bridge remains relatively unchanged, and the charges on the $\text{Li}^1\text{--Cl--Li}^2\text{--C}^4\text{H}_3$ moiety show very little change ($< \pm 0.04$, data not shown).

The structure of the propenyl cuprate **PD** at the MP2 level of theory was essentially the same as that for the HF structure and show close resemblance to the calculated^{11,55} and crystal structures of dimeric lithium cuprate clusters of general structure **A** (as later described in the Appendix).¹⁰ The C--Cu bond lengths show close agreement ($\pm 3\text{--}7\%$) with experimental values for the related structure.^{11,55} **PD** features the $\text{C}^1\text{--Cu}$ σ -bonding and π -coordination between Li^1 and C^1 , resembling the geometry found in the crystal of $\{[\text{Li}(\text{OEt}_2)]_2\text{Cu}(\text{C}_6\text{H}_5)_2\}_2$.^{10b}

2. B3LYP Studies. Stationary points obtained by the MP2 method was examined also by the B3LYP method. Thus, **CP**, **TS**, and **PD** in the $\text{Me}_2\text{CuLi}\cdot\text{LiCl}$ reaction were optimized at the B3LYP/631A level (Figure 8B). The B3LYP/631A structures were indeed found to be in good agreement with the MP2/631WH structure (Figure 8A). The B3LYP/631A bond lengths reproduced those obtained by the MP2/631WH within 2%, except for some partial bonds (dotted line) which were off by $< 10\%$. It is reported that relativistic effect for copper atom is the largest among first row transition metals.⁷¹ Hence, we evaluated the relativistic effects on the copper atom at the B3LYP/631D level (Figure 8C) to find that the difference of the bond length between the B3LYP/631A and the B3LYP/631D methods was less than 1.7%.

The activation energy at the B3LYP/631A//B3LYP/631A level is 13.6 kcal/mol. The relativistic effect on the activation energy is comparable (12.7 kcal/mol at the B3LYP/631D//B3LYP/631D). Though these activation energies are rather unrealistically small, they are somewhat closer to the best estimated activation energy of 19.1 kcal/mol (CCSD(T)/631WH//MP2/631WH, vide supra) than the MP2/631WH energy (26.6 kcal/mol). The energetics of the $\text{Me}_2\text{CuLi}\cdot\text{LiCl}$ reaction is shown in Figure 9 and may be compared with the data of other reactions studied at the same level of theory.

(Me_2CuLi)₂ Addition. The reaction of the dimer (Me_2CuLi)₂ was next examined for three important stages of the reaction, **RT1-d**, **CP-d**, and **TS-d** (Figure 11), and surprising similarity was found with $\text{Me}_2\text{CuLi}\cdot\text{LiCl}$. Most importantly, the spatial arrangement of the crucial $\text{Li}^1\text{--C}^1\text{--C}^2\text{--Cu}^1\text{--C}^3\text{--C}^4$ moiety of these three stationary points remains essentially the same as that obtained for the monomer (Figure 8) with only 0–3.8% differences of the bond lengths (compared at the B3LYP/631A level). The activation energy for (Me_2CuLi)₂ (16.1 kcal/mol,

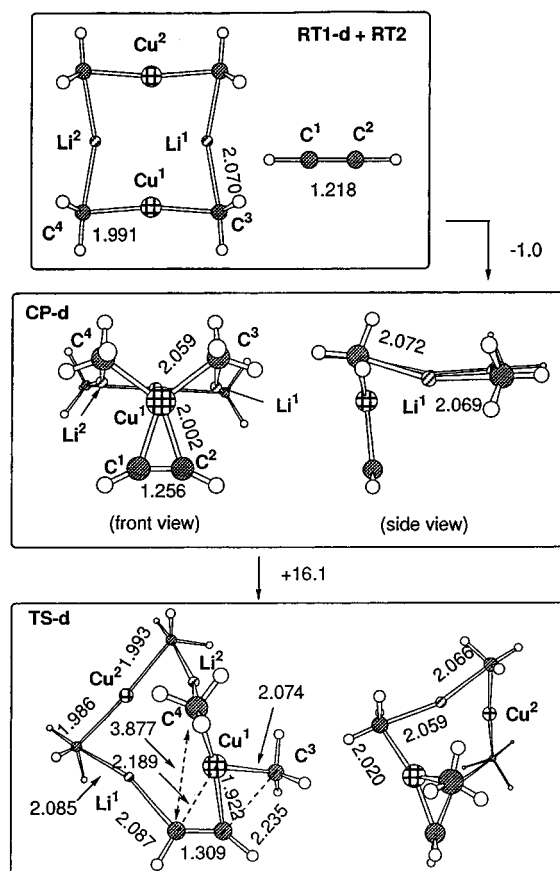


Figure 11. Reactants, complex, **TS** in the reaction of (Me_2CuLi)₂ with acetylene. Bond lengths and angles at the B3LYP/631A level are shown in Å and deg, respectively. Energy changes at the B3LYP/631A/B3LYP/631A level are shown on the arrows in kcal/mol. The value of imaginary frequency of **TS-d** is $272.8i\text{ cm}^{-1}$.

B3LYP/631A//B3LYP/631A) was found to be higher than the 13.6 kcal/mol value for $\text{Me}_2\text{CuLi}\cdot\text{LiCl}$ (B3LYP/631A//B3LYP/631A). The lower activation energy in the latter is perhaps due to better charge stabilization by the Li^1 atom which is attached to the electronegative chlorine atom.

Discussion

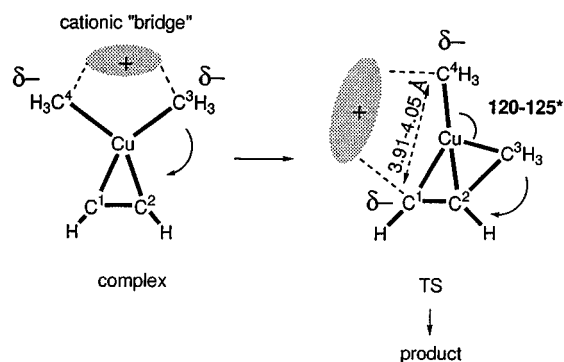
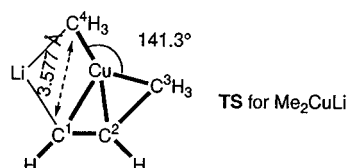
The above results represent the first computational simulation of the reaction pathway of a large polymetallic cuprate cluster with acetylene. All stationary points **CP**, **TS**, and **PD** in Scheme 4 have been structurally correlated by the IRC reaction-path-following method and the usual geometry optimization procedure. We first compared the noncluster copper compounds and the lithium organocuprate clusters and then evaluated the effects of cluster structure for $\text{Me}_2\text{CuLi}\cdot\text{LiCl}$ and (Me_2CuLi)₂.

Simple organocuprate reagents (RCu) are unreactive reagents, while organocuprate reagents (R_2CuM) are reactive for the delivery of a nucleophilic R group to acetylene and cyclopropene. When the counteraction M^+ is removed by solvation, the remaining R_2Cu^- loses its nucleophilicity. As shown in Figures 2, 4, 6, 9, and 11, the calculated activation energies (B3LYP/631A//B3LYP/631A) of the addition of various organocuprate reagents to acetylene depends very much on the nature of the reagents. Of the five cuprate structures examined, the energies of MeCu and Me_2CuLi are anomalous, while others show a similar trend. The origins of the anomalies for MeCu and the minimum cluster Me_2CuLi were discussed above.

The activation energy of the MeCu addition to acetylene is very high (43.6 kcal/mol, B3LYP/631A//B3LYP/631A). The

(71) Pyykkö, P. *Chem. Rev.* **1988**, *88*, 563–594.

Scheme 5

(a) Geometries of the "core" portion for Me_2Cu^- , $\text{Me}_2\text{CuLi}\cdot\text{LiCl}$, $(\text{Me}_2\text{CuLi})_2$ (b) Geometry of the "core" portion for Me_2CuLi 

metal center is acting as a Lewis acid, and the direct cleavage of the covalent C—Cu bond (estimated to be 55 kcal/mol)⁷² contributes to the high energy barrier. In the reaction of Me_2Cu^- with acetylene, a back-donation process as well as donative interaction operates to cause charge transfer from the cuprate to acetylene. The activation energy drops by 23 kcal/mol to become 20.3 kcal/mol (B3LYP/631A//B3LYP/631A). When Me_2Cu^- is incorporated as part of a lithium cuprate cluster, the activation energy decreases further to become 13.6–16.1 kcal/mol (B3LYP/631A//B3LYP/631A). The activation energy is estimated to be 19.1 kcal/mol at the CCSD(T)/631WH level (vide supra), and this value is reasonable for a reaction taking place below 0 °C (Table 2).

It is notable that the basic atomic arrangement found in the complex and the TS of the reaction of Me_2Cu^- (cf. Figure 4 and heavy lines in Scheme 5a) is found largely unchanged in the corresponding structures in the reactions of all the lithium cuprate clusters, except for that of the minimum cluster Me_2CuLi (Scheme 5b). This similarity leads to a reasonable assumption that the geometry of atoms surrounding the copper atom is controlled mainly by copper's coordination geometry and rather little by the other atoms in the cuprate cluster. Thus, the "bridge" structure ($\text{Li}^1\cdot\text{Li}^2$), which is large enough to fill in the distance of 3.9–4.05 Å between C^1 and C^4 atoms, stabilizes well the two negatively charged sites. In the minimum cluster, Me_2CuLi , the single Li cation is apparently so small that it can only achieve stabilization by changing the geometry of the "core structure". The electronic property of the bridge will also contribute to the charge stabilization. With its chlorine atom, the Li—Cl—Li bridge should be a better negative charge stabilizer than the Li—Me—Cu—Me—Li, and this could be a reason for the lower activation energy for $\text{Me}_2\text{CuLi}\cdot\text{LiCl}$. One recognizes that the TS becomes earlier (longer $\text{C}^2\text{—C}^3$ bond, and shorter $\text{C}^2\text{—Cu}$ bond) as the activation energy decreases in the order of $(\text{Me}_2\text{CuLi})_2$, Me_2CuLi , and $\text{Me}_2\text{CuLi}\cdot\text{LiCl}$.

The role of the counter cation (M^+) in R_2CuM is summarized in the conceptual sketch shown in Scheme 6. Thus, the cuprate anion first donates electrons to acetylene ($d\text{-}\pi^*$ interaction), and the countercation participates in the stabilization of the negative

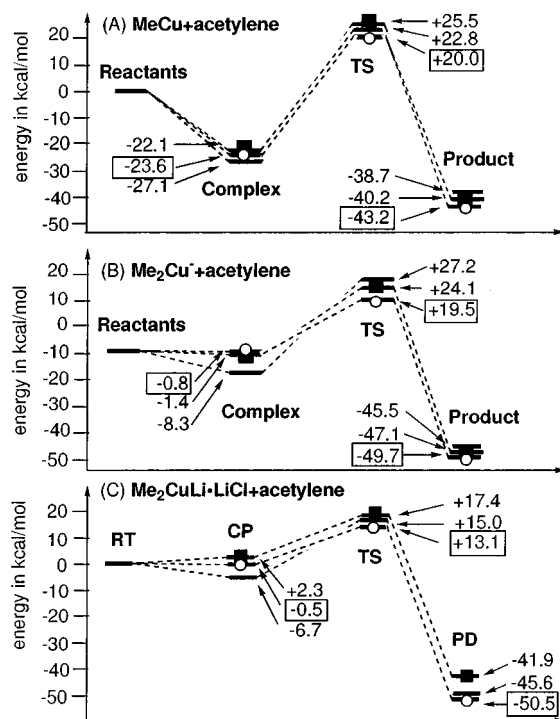
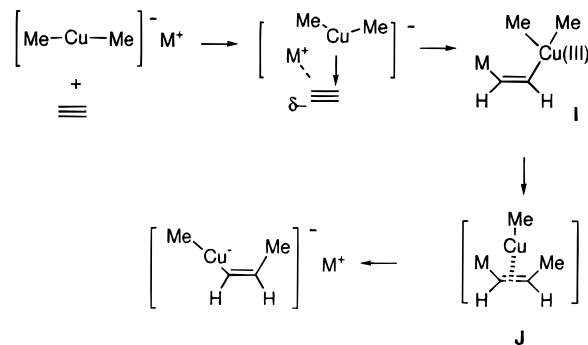


Figure 12. Potential energy profiles of (A) MeCu , (B) Me_2Cu^- , and (C) $\text{Me}_2\text{CuLi}\cdot\text{LiCl}$ addition to acetylene at various levels. Bars with white circles are at the CCSD(T)/631WH//B3LYP/631A level (A, B) or at the CCSD(T)/321A//B3LYP/631A level (C), and with black squares are at the B3LYP/631A//B3LYP/631A level. The others are at the MP2/631WH//B3LYP/631A level. Energies relative to reactants in kcal/mol are shown near arrows. The energies with box are at the B3LYP/631A level.

Scheme 6



charge to generate **I** (depicted as an extreme representation). This species is unstable (which is in fact a TS as shown in the present studies) and undergoes reductive elimination to generate a vinyl metallic species **J** and MeCu . Intracuster transmetalation affords a vinylcuprate product. The low reactivity of the crown-solvated R_2CuLi strongly suggests that M^+ must exist better as a part of the cuprate cluster.

The above data provide a unified mechanism for the puzzling behavior of the propargylic acetate and methyl ether in Schemes 2 and 3.^{32,34b} According to the above mechanistic framework, the initial stage of the reaction will involve reversible electron donation from the cuprate to the substrate (**K** in Scheme 7). When there is a good leaving group such as acetate, electron donation at the acetylene terminus will kick out the leaving group to generate an allenyl Cu(III) species **L**, which then gives the allene upon reductive elimination. When the leaving group is a less potent methoxy group (Scheme 7b), the standard sequence of carbocupration takes place (via **M** as an unstable intermediate) to generate a stable vinyl cuprate (**O**), which then

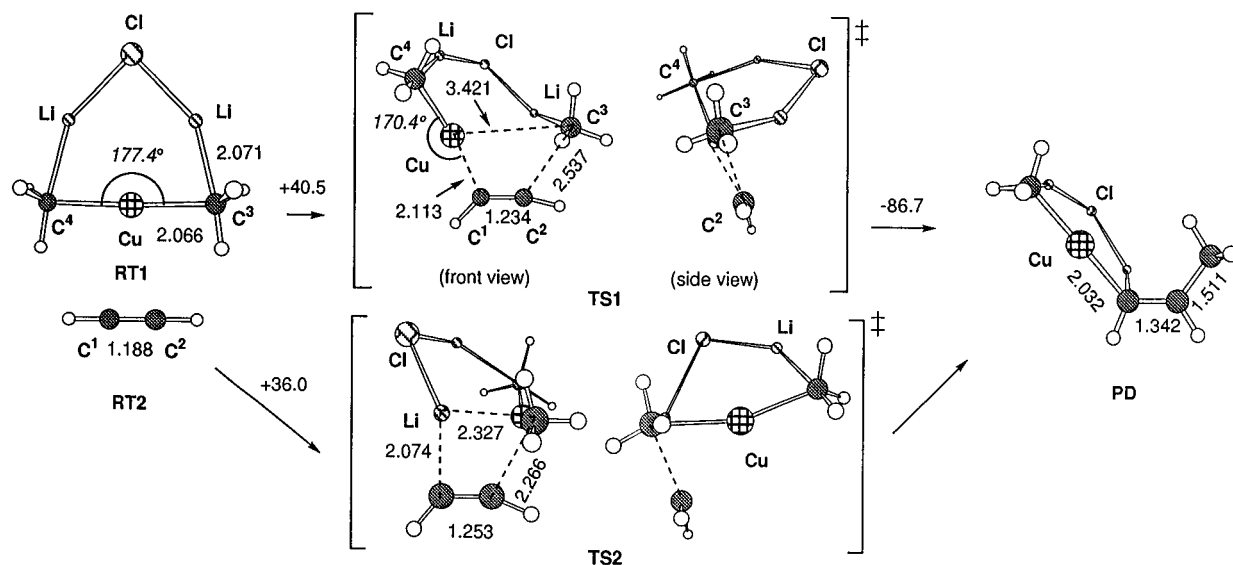
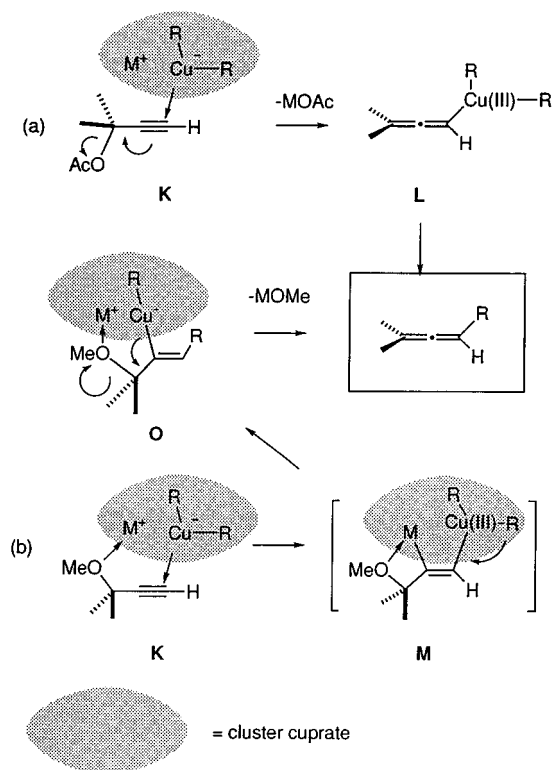


Figure 13. Representative structures in the $\text{Me}_2\text{CuLi}\cdot\text{LiCl}$ addition to acetylene at the HF/631WH level. Bond lengths and angles are shown in Å and deg, respectively. Energy changes at the HF/631WH level are shown on the arrows in kcal/mol. Total energy of sum of **RT1** and **RT2** is -2269.39625 hartree (HF/631WH/HF/631WH).

Scheme 7



undergoes 1,2-elimination. Clearly, the first pathway (Scheme 7a) has much to do with the mechanism of $\text{S}_{\text{N}}2'$ -substitution reaction.^{5,73}

The studies in this and the following paper revealed that the essence of the C–C bond forming reaction is remarkably insensitive to the difference of cluster structures. In both $\text{Me}_2\text{CuLi}\cdot\text{LiCl}$ and $(\text{Me}_2\text{CuLi})_2$ clusters, lithium atom followed later by bond reorganization involving the cleavage of labile C–Cu(I) bond. In this way, the reaction circumvents the high energy cost of direct C–Cu(I) bond cleavage (55 kcal/mol).⁷² As the electron donation to acetylene takes place, the copper(I) atom loses electrons to form a copper(III) transition species, which immediately starts to undergo reductive elimination without

forming a stable intermediate. The negative charge is transferred from the copper 3d orbital, and the transferred charge becomes stabilized by the lithium atom (Li^+), as shown by **LMO3** and **LMO4** in Figure 10. The whole reaction pathway illustrates the uniqueness of copper among neighboring elements in the Periodic Table for its two-stage redox properties and its ability to form a stable ate complex cluster. The $\text{Li}^+\cdot\text{Li}^2$ bridge structure of reasonable size not only stabilizes the starting cluster but also assists the electron flow during C–C bond formation. The M^+ and LiX in R_2CuM and $\text{R}_2\text{CuM}\cdot\text{LiX}$ are therefore active participants of the reaction.

In summary, the present studies show that lithium organocuprate clusters have a built-in function to facilitate carbocupration reactions, which is not available for noncluster copper reagents (RCu and R_2Cu^-). In light of its predominance in a solution of a standard Gilman reagent, the dimeric cluster $(\text{Me}_2\text{CuLi})_2$ is a good candidate for the reactive species, as has been widely believed. On the other hand, the close similarity of $\text{Me}_2\text{CuLi}\cdot\text{LiCl}$ and $(\text{Me}_2\text{CuLi})_2$ suggests that the LiX -complexed species ($\text{Me}_2\text{CuLi}\cdot\text{LiX}$) and various other higher homologues can also act as reactive species if they have a suitably structured bridge and high equilibrium concentration. The minimum cluster Me_2CuLi species is a less likely reactive species because of its low equilibrium concentration. The importance of the Cu(I)/Cu(III) redox process and the active role of M^+ as counteraction was also found in the conjugate addition described in the following article. On the basis of the above results, we can ascribe the uniqueness of the copper atom to its ability to easily undergo the Cu(I)/(III) redox process as well as to form stable polyorgano polymetallic ate complexes. No elements in the neighborhood of copper in the Periodic Table possess these two properties together.

Appendix: Comparison of the Theoretical Methods

In this Appendix, the performance of theoretical methods is described for the geometries of simple organocuprate compounds and for the energetics of stationary points in the MeCu and Me_2Cu^- additions. Overall, the B3LYP geometry reproduces the MP2 geometry, and the B3LYP energetics is closer to the CCSD(T) data than the MP2 energetics.

1. Comparison for Stable Structures. Comparison of the theoretical methods for the stable structures is summarized in

(72) Armentrout, P. B.; Georgiadis, R. *Polyhedron* **1988**, *7*, 1573–1581.

Table 1. Among the C–Cu bond lengths obtained for the linear cuprate anion Me–Cu–Me[−], the HF/631WH value (2.066 Å) is 6% longer than that of the experimental data (1.935 Å),⁵⁴ to which the values at the MP2/631WH (1.929 Å), B3LYP/631A (1.969 Å), and values in previous MP2^{43,74} and DFT^{55,75} results are close. The optimized structure of Me₂CuLi·LiCl (**RT1**) was found to be very similar to those obtained for LiI, LiCN, and MeLi complexes.^{11,55} The calculated structures of (Me₂CuLi)₂ (**RT1-d**) and [Me₂CuLi(H₂O)]₂ (**RT1w**) were reported previously.^{11,43} Other structural data are summarized in Table 1, which shows that B3LYP method reasonably reproduces the MP2 geometry.

2. Comparison for Intermediates and TSs. The energetics of the reaction intermediates of MeCu, Me₂Cu[−], and Me₂CuLi·LiCl additions to acetylene were also examined. The potential energy profiles calculated at the MP2/631WH, B3LYP/631A, and CCSD(T)/631WH (for Me₂CuLi·LiCl addition, CCSD(T)/321A used) levels for B3LYP/631A optimized geometries are shown in Figure 12.

It can be seen that the MP2 complexation energies tend to be larger than the CCSD(T) ones and that the B3LYP ones smaller than the latter. Reverse situation is found for the energies of the TSs. Hence the MP2 activation energies are always larger than the B3LYP ones.

3. HF Studies on the Reaction of Me₂CuLi·LiCl. Studies on the cuprate reactivities in the Me₂CuLi·LiCl reaction (Figure 13) were performed at the HF level to find that this level of calculations is not suitable for the studies of the TSs.

The TS of C–C bond formation (**TS1**) was characterized by its single negative frequency (532.2i cm^{−1}) corresponding to the C²–C³ bond formation (Figure 13). The C¹–Cu–C⁴ bond is in a near linear arrangement and the C³–Cu bond is totally cleaved. The TS hence represents the TS for direct insertion of acetylene to the C–Cu bond. Going down the energy hill along the IRC, the TS went smoothly to the desired product **PD** with 86.7 kcal/mol exothermicity, which confirms that **TS1** lies on the HF potential surface leading to C–C bond formation. On the other hand, we followed the IRC from **TS** toward the reactants and could not find such a π -complex as found in the higher level calculations.

The vinyl cuprate product **PD** is a mixed cluster composed of MeLi, LiCl, and CH₃CH=CHCu and is similar to **RT1** for the fundamental cyclic structure. The HF structure was found to be very similar to that found at the MP2 level (vide infra).

The energy difference between the reactants and **TS1** is unrealistically high (40.5 kcal/mol, HF/631WH//HF/631WH) and even increased to 42.3 kcal/mol at the MP2/631WH//HF/631WH level, indicating that **TS1** cannot exist on the MP2 potential surface. We also searched for other possibilities to find the second TS (**TS2**) which is a TS of acetylene insertion into the weaker Me–Li bond leading to formal MeLi addition. The energy of the TS is 36.0 kcal/mol (HF/631WH//HF/631WH), which is still too high.

In summary, both *ab initio* MP2 and density functional B3LYP methods give reasonable geometric data, yet the MP2 method overestimates the activation energy of the C–C bond formation where the nature of the copper/acetylene complexation changes dramatically.

Experimental Details for Eq 2. Carbocupration in the Absence of 12-crown-4 (a Control Experiment). To a suspen-

sion of CuI (52.3 mg, 0.275 mmol) in dry ether (4.5 mL) was added a 1.55 M hexane solution of *n*-BuLi (0.355 mL, 0.55 mmol) at −40 °C over 5 min. Resulting black solution was stirred at −25 °C for 30 min and then cooled to −40 °C again. Phenylacetylene (55.0 μ L, 0.50 mmol) was added to the solution of the cuprate at that temperature, and the reaction mixture was stirred at 4 h and then quenched with saturated aqueous NH₄Cl. The reaction mixture was diluted with Et₂O and passed through a pad of silica gel. Evaporation of solvent *in vacuo* afforded a pale yellow oil. Silica gel chromatography (silica gel 2.0 g, pentane) afforded a mixture of linear and blanched (cf. eq 2) carbocupration products as a colorless oil (53.3 mg, 0.28 mmol, 56% yield).

Carbocupration in the Presence of 10 Equiv of 12-crown-

4. To a suspension of CuI (31.4 mg, 0.165 mmol) in dry ether (2.7 mL) was added a 1.55 M hexane solution of *n*-BuLi (0.215 mL, 0.167 mmol) at −40 °C over 5 min. Resulting black solution was stirred at −25 °C for 30 min and 12-crown-4 (0.53 mL, 3.3 mmol) was added dropwise. The resulting charcoal gray suspension was stirred for an additional 30 min and then cooled to −40 °C again. Phenylacetylene (32.9 μ L, 0.3 mmol) was added to the suspension at that temperature, and the reaction mixture was stirred for 4 h and then quenched with saturated NH₄Cl. After workup as mentioned above, silica gel chromatography (silica gel 1.0 g, pentane) afforded a 85:15 mixture of linear and blanched carbocupration product as a colorless oil (5.9 mg, 0.031 mmol, 12.3% yield). Upon running the reaction further at −20 to 0 °C for 18 h, we obtained the product in 53% yield. The rate retardation effect of the crown ether was also observed, when *n*-BuLi was treated first with the crown ether before preparation of the cuprate reagent. Physical data for the carbocupration product: IR (neat, a 91:9 mixture of regio isomers) 2656.3, 2927.4, 2861.8, 1625.7, 1492.6, 1456.0, 1378.9, 1261.2, 1095.4, 1025.9, 894.8, 777.1, 700.0; ¹H NMR (400 MHz, CDCl₃, major isomer) δ 0.89 (t, *J* = 7.08 Hz, 3 H), 1.29–1.51 (m, 4 H), 2.50 (br t, *J* = 7.57 Hz, 2 H), 5.05 (br s, 1 H), 5.25 (br s, 1 H), 7.2–7.5 (m, 5 H); ¹H NMR (400 MHz, CDCl₃, minor isomer); δ 0.92 (t, *J* = 7.0 Hz, 3 H), 1.29–1.51 (m, 4 H), 2.20 (dt, *J* = 7.0, 14.5 Hz, 2 H), 6.22 (dt, *J* = 6.9, 16.0 Hz, 1 H), 6.37 (distorted br d, *J* = 16.0 Hz, 1 H), 7.2–7.5 (m, 5 H); ¹³C NMR (100 MHz, CDCl₃, major isomer) δ 13.91, 22.41, 30.46, 35.07, 112.00, 126.10 (2 C), 127.20, 128.21 (2 C), 128.44, 148.76. Elemental analysis (for a 91:9 mixture of regio isomers) calcd for C₁₂H₁₆: C, 89.94; H, 10.06. Found: C, 90.21; H, 9.79.

Acknowledgment. We thank Prof. B. H. Lipshutz for helpful discussion and Dr. M. Isaka for provision of some experimental data. Financial support from the Ministry of Education, Science and Culture, Japan to E.N. and from the National Science Foundation to K.M. is gratefully acknowledged. E.N. thanks the generous allotment of computer time from the Institute for Molecular Science, Japan. S.M. thanks JSPS for a predoctoral fellowship.

Supporting Information Available: Cartesian coordinates of stationary points in the MeCu, Me₂Cu[−], and Me₂CuLi addition (B3LYP/631A), and **CP**, **TS**, **PD**, **CP-d**, and **TS-d** at the MP2/631WH and B3LYP/631A levels (10 pages). See any current masthead page for ordering and Internet access instructions.

JA964208P

(73) Anderson, R. J.; Hendrick, C. A.; Siddall, J. B. *J. Am. Chem. Soc.* **1970**, *92*, 735–737. Anderson, R. J. *J. Am. Chem. Soc.* **1970**, *92*, 4978–4979. Herr, R. W.; Johnson, C. R. *J. Am. Chem. Soc.* **1970**, *92*, 4979–4981.

(74) Antes, I.; Frenking, G. *Organometallics* **1995**, *14*, 4263–4268.

(75) Sosa, C.; Andzelm, J.; Elkin, B. C.; Wimmer, E.; Dobbs, K. D.; Dixon, D. A. *J. Phys. Chem.* **1992**, *96*, 6630–6636.